Chapter 2
Stress Distribution in Elastic Plane with a Semi-infinite Notch

Abstract The second chapter presents analysis of stress fields in elastic plane with a semi-infinite notch under conditions of plane stress state or plane strain state. Well-known boundary value problem solutions for eigenvalues of a wedge in the plane elasticity theory are considered at first. Then the same solutions are constructed for the semi-infinite rounded V-shaped notch. Based on these solutions, the relationship between stress concentration factor and stress intensity factor in elastic bodies with rounded or sharp V-shaped notches had been established.

2.1 Methods for Stress Analysis in Notched Bodies

Studies of stress and displacement fields around tip of sharp V-notch with different boundary conditions given at its edges are of great importance in fracture mechanics. Investigations in this field had been initiated by Wieghardt [242] as far back as in year 1907. In the thirties of the last century, they were continued by Brahtz [25–27]. In 1952, Williams [243] had studied the eigenvalues problem for elastic wedge with various boundary conditions given at its edges. Thereafter these issues had been examined by many other researchers [11, 13, 44, 96, 105, 106, 182, 187, 208, 216, 218, 222, 244]. Bodies with V-notches, just as bodies with cracks, are classified in fracture mechanics in relation to loading mode (Fig. 2.1). Namely, there is Mode I, when tensile loads are applied symmetrically with respect to bisector plane, and Modes II or III, when shear loads are applied antisymmetrically in relation to bisector plane and directed either perpendicular or parallel to notch front (hereinafter term "front" designates the intersection of V-notch's faces, whereas term "edge" corresponds to divergent projections of wedge, just in the case of crack). First two loading modes are created by forces applied to the body with V-notch in the plane that is perpendicular to notch front. These modes will be studied in this chapter within a plane problem of elasticity theory. The third loading mode is created by forces parallel to notch front and called out-of-plane or antiplane shear. This mode will be considered in Chap. 10.

M.P. Savruk and A. Kazberuk, *Stress Concentration at Notches*,
DOI 10.1007/978-3-319-44555-7_2

Stresses in elastic body with V-notch can be presented in the form

$$\sigma_{ik} = \frac{\tilde{K}_{\mathrm{I}}^{\mathrm{V}}}{(2\pi r)^{\lambda_{\mathrm{I}}}} f_{ik}(\beta,\theta) + \frac{\tilde{K}_{\mathrm{II}}^{\mathrm{V}}}{(2\pi r)^{\lambda_{\mathrm{II}}}} g_{ik}(\beta,\theta) + \frac{\tilde{K}_{\mathrm{III}}^{\mathrm{V}}}{(2\pi r)^{\lambda_{\mathrm{III}}}} h_{ik}(\beta,\theta) \quad (i,k = r,\theta,z), \qquad (2.1)$$

where $\tilde{K}_{\mathrm{I}}^{\mathrm{V}}$, $\tilde{K}_{\mathrm{II}}^{\mathrm{V}}$, and $\tilde{K}_{\mathrm{III}}^{\mathrm{V}}$ are stress intensity factors (generalized) in the tip of V-notch with opening angle 2β; λ_{I}, λ_{II}, and λ_{III} are stress singularity exponents; (r,θ) are polar coordinates with pole in notch tip and polar axis along axis x (see diagram in Fig. 2.1).

The presence of power singularity in elastic body essentially complicates numerical solution of elasticity theory's boundary value problems for regions with notched boundary. It is especially true for problems, in which mixed loading modes (I+II modes) are realized, i.e., simultaneously two different singularities arise near notch tip. Therefore numerical analysis often relies on approximate approaches, which either ignore singularities in corner points at all or consider only a single singularity of higher order [77, 116].

For the first time, stress intensity factor in the tip of sharp edge notch in a rectangular specimen under tension and bending was determined using a method of boundary collocations [85]. In order to do so, a known [243] expansion into an eigenfunction series within an elasticity theory plane problem for a wedge was used. Expansion coefficients were determined from algebraic equations system, which was constructed by obeying boundary conditions in a respective number of collocation points. Such approach was proved to be effective at vertex angles $2\beta < \pi/3$. At larger vertex angles, it was necessary to take number of collocation points higher than required to determine coefficients of truncated series, i.e., number of constructed algebraic equations was higher than number of unknown functions. In such cases complete equations system were constructed using a least squares method [31, 32].

To solve two-dimensional problems of elasticity theory in notched regions, the finite elements method (FEM) is most appropriate. This method is based on application of special finite elements, which allow describing desired stress field singularity using asymptotic analytical solutions. Such special elements surround the singularity

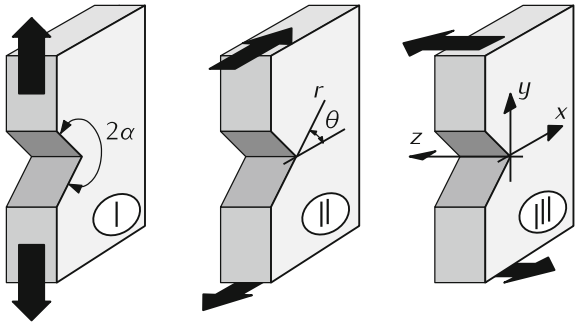

Fig. 2.1 Three loading modes for a body with V-notch

in the body's boundary (notch vertex). There are three groups of such finite elements in use: hybrid elements (see, e.g., [141]), degenerated asymptotic elements [1], and analytical elements [219].

Stress intensity factors are determined using few different approaches as well [218, 221]. There are direct methods [141, 217, 219], which yield SIF values immediately from simulated stress field near notch tip; asymptotic methods [213], which compare stress distributions in vicinity of singularity obtained both analytically and numerically, and energy methods [10, 16, 29, 30, 37, 43, 142, 143, 180, 226, 227, 230, 256–258], which use energy integrals independent of integration path.

Overviews of studies in notched bodies fracture mechanics performed on the basis of finite elements method can be found in monographs [216, 218] and papers [70, 79, 80, 215, 217, 222, 259].

Another approach, frequently used in solving problems of elasticity theory for bodies with notches, is boundary element method (BEM) [44, 58, 84, 123, 171, 173, 174, 218, 238, 251]. In boundary element approach, only region's boundaries are discretized. However, description of stress singularity at the sharp notch vertex here requires use of special boundary elements similarly to finite elements approach. Some numerical methods [71–73, 168, 231, 232] use boundary elements or boundary collocation to construct up weighting functions as well. Such functions enable calculating stress intensity factors at the sharp notch or notch crack tip under any type of loading based merely on integration of stresses at boundary of body with corresponding weighting functions. It should be noted that the method of weighting function has found only limited application in solving problems of elastic regions with notches.

More frequently used in stress concentration problems is so-called body force method [157, 158]. Applications of this method in solving problems of stress concentration near notches are reviewed in publications [42, 161].

We shall use in present work the method of singular integral equations [188] to solve two-dimensional problems of elasticity theory. This method allows directly determining stress intensity factors for any systems of straight [165] or curvilinear [188] cracks as well as analyzing stress distributions in complicated regions with holes and/or notches [208] or elastic inclusions [207]. One of the first problems solved using this method was SIF calculating in the tip of edge V-notch in elastic half-plane [234], integral equation of the problem being derived for a system of arbitrarily oriented straight cracks in half-plane [191]. The method of singular integral equations had proved to be especially effective in elastic regions with smooth boundary. Numerical implementation of this method encounters essential difficulties for regions with corner points in boundary contours including regions with V-notches [2, 12, 55, 69, 76, 92, 93, 147, 149, 150, 171, 172, 186, 190, 206, 208, 262–264]. A unified approach was developed for regions with V-notches [107–115, 166, 192–205, 210–212] consisting in SIF determining in sharp notch tip using data on stress concentration in tips of corresponding rounded V-notches.

Fracture mechanics includes also problems concerning stress concentration near V-notches with strongly rounded tips, which generate very high stresses (higher than ultimate strength of material) even at small loads and prevents from strength

estimating from classical criteria. Studies in this field are very rare that can be explained by analytical difficulties arising in solving problems of elasticity theory for bodies with rounded V-notches with small radii of curvature in tips. To solve problems of such class starting from data on stress concentration in the rounded V-notch tip with a quite large radius of curvature, approximate methods are therefore of great importance. Such data can be collected by various techniques. To find a solution, one must know how stress concentration factor for rounded notch tip with a small radius of curvature asymptotically depends on stress intensity factor for similar sharp stress concentrator. These dependencies can be obtained by solving the singular boundary value problem of semi-infinite rounded V-shaped notch in elastic plane under ordinary asymptotic conditions for a stress field at infinity [15, 45, 46]. To construct solutions to such problems we used the method of singular integral equations.

2.2 Eigensolutions of Elasticity Theory Plane Problem for Wedge

2.2.1 Characteristic Equations

Let us study the eigenvalues problem for elastic wedge occupying the region $S = \{(r, \theta);\ r \geq 0,\ -\alpha \leq \theta \leq \alpha\}$, where r, θ are polar coordinates with pole in wedge tip and polar axis along wedge bisector: $z = x + \mathrm{i}y = r\mathrm{e}^{\mathrm{i}\theta}$ (Fig. 2.2).

Both normal ($\sigma_{\theta\theta}$) and shear ($\tau_{r\theta}$) stresses at wedge faces are absent

$$\sigma_{\theta\theta} + \mathrm{i}\tau_{r\theta} = 0, \qquad \theta = \pm\alpha. \tag{2.2}$$

Stress state inside the wedge is expressed in terms of complex stress potentials $\Phi(z)$ and $\Psi(z)$ using formulae [153]

$$\begin{aligned} \sigma_{rr} + \sigma_{\theta\theta} &= 2\left[\Phi(z) + \overline{\Phi(z)}\right], \\ \sigma_{rr} - \mathrm{i}\tau_{r\theta} &= \Phi(z) + \overline{\Phi(z)} - z\Phi'(z) - \frac{z}{\overline{z}}\Psi(z). \end{aligned} \tag{2.3}$$

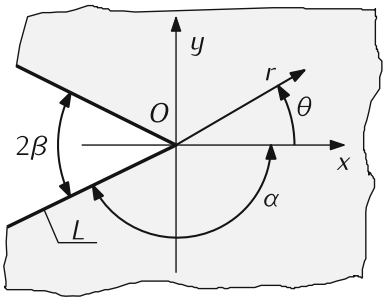

Fig. 2.2 Elastic wedge with vertex angle 2β

We are seeking the complex stress potentials in the form

$$\Phi(z) = Az^{-\lambda}, \qquad \Phi(z) = Bz^{-\lambda}, \tag{2.4}$$

where A, B are complex constants. Although parameter λ can be, in general, complex, we shall assume for simplicity this parameter λ real. It was shown earlier [244] that the same result can be obtained even without such restriction, i.e., seeking complex potentials in the form

$$\Phi(z) = Az^{-\lambda} + A'z^{-\overline{\lambda}}, \qquad \Phi(z) = Bz^{-\lambda} + B'z^{-\overline{\lambda}}, \tag{2.5}$$

where A, B, A', B' are complex constants. It follows from energy considerations (the condition of energy integral finiteness) that the parameter λ must obey the condition $\lambda < 1$ (or Re $\lambda < 1$) [11, 239, 240].

From equalities (2.3) one derives

$$\sigma_{\theta\theta} + \mathrm{i}\tau_{r\theta} = \Phi(z) + \overline{\Phi(z)} + z\Phi'(z) + \frac{z}{\overline{z}}\Psi(z). \tag{2.6}$$

Now write the homogeneous equations system based on boundary conditions

$$\begin{aligned} A\mathrm{e}^{-\mathrm{i}\lambda\alpha}(1-\lambda) + \overline{A}\mathrm{e}^{\mathrm{i}\lambda\alpha} + B\mathrm{e}^{\mathrm{i}\alpha(2-\lambda)} &= 0, \\ A\mathrm{e}^{\mathrm{i}\lambda\alpha}(1-\lambda) + \overline{A}\mathrm{e}^{-\mathrm{i}\lambda\alpha} + B\mathrm{e}^{-\mathrm{i}\alpha(2-\lambda)} &= 0. \end{aligned} \tag{2.7}$$

Supplement this system with two more adjoint equations

$$\begin{aligned} A\mathrm{e}^{-2\mathrm{i}\lambda\alpha}(1-\lambda) + \overline{A} + B\mathrm{e}^{2\mathrm{i}\alpha(1-\lambda)} &= 0, \\ A\mathrm{e}^{2\mathrm{i}\lambda\alpha}(1-\lambda) + \overline{A} + B\mathrm{e}^{-2\mathrm{i}\alpha(1-\lambda)} &= 0, \\ A + \overline{A}\mathrm{e}^{2\mathrm{i}\lambda\alpha}(1-\lambda) + \overline{B}\mathrm{e}^{-2\mathrm{i}\alpha(1-\lambda)} &= 0, \\ A + \overline{A}\mathrm{e}^{-2\mathrm{i}\lambda\alpha}(1-\lambda) + \overline{B}\mathrm{e}^{2\mathrm{i}\alpha(1-\lambda)} &= 0. \end{aligned} \tag{2.8}$$

In order for existence of nontrivial solution of homogeneous equations system, its determinant must be zero.

$$\begin{vmatrix} \mathrm{e}^{-2\mathrm{i}\lambda\alpha}(1-\lambda) & 1 & \mathrm{e}^{2\mathrm{i}\alpha(1-\lambda)} & 0 \\ \mathrm{e}^{2\mathrm{i}\lambda\alpha}(1-\lambda) & 1 & \mathrm{e}^{-2\mathrm{i}\alpha(1-\lambda)} & 0 \\ 1 & \mathrm{e}^{2\mathrm{i}\lambda\alpha}(1-\lambda) & 0 & \mathrm{e}^{-2\mathrm{i}\alpha(1-\lambda)} \\ 1 & \mathrm{e}^{-2\mathrm{i}\lambda\alpha}(1-\lambda) & 0 & \mathrm{e}^{2\mathrm{i}\alpha(1-\lambda)} \end{vmatrix} = 0. \tag{2.9}$$

From here we come to the characteristic equation

$$(1-\lambda)^2 \sin^2 2\alpha - \sin^2(2\alpha(1-\lambda)) = 0, \tag{2.10}$$

which decomposes onto two equations: for symmetrical [243]

$$(1-\lambda)\sin 2\alpha + \sin(2\alpha(1-\lambda)) = 0 \tag{2.11}$$

and antisymmetrical [243]

$$(1-\lambda)\sin 2\alpha - \sin(2\alpha(1-\lambda)) = 0 \tag{2.12}$$

stress distributions with respect to wedge bisecting line.

Equations (2.11) and (2.12) in the interval $0 < \mathrm{Re}\,\lambda < 1$ have no roots for $0 < \alpha < \pi/2$, whereas for $\pi/2 < \alpha < \pi$ each of these equations has one real root λ_{I} (symmetrical configuration) and λ_{II} (antisymmetrical configuration), which belong to the interval $(0,\ 1/2)$. At $\alpha = \pi$ (semi-infinite crack) these roots coincide: $\lambda_{\mathrm{I}} = \lambda_{\mathrm{II}} = 1/2$. Numerical values of stress singularity exponents λ_{I} and λ_{II} are presented in Tables 2.1 and 2.2.

Symmetrical stress distribution has a power singularity of order λ_{I} for V-notches with vertex angle $0 \le 2\beta < \pi$ $(\pi < 2\alpha \le 2\pi)$. Antisymmetrical stress distribution has a power singularity of order λ_{II} for V-notches with vertex angle $0 \le 2\beta < 2\beta^*$. Here angle $\beta^* = 0.894888$ (51.2733°) is the root of equation

$$\tan 2(\pi - \beta) = 2(\pi - \beta), \tag{2.13}$$

which can be obtained from equality (2.12), if the parameter λ_{II} approaches zero [11, 28, 236]. Dependence of stress singularity exponents in the tip of V-notch λ_{I} and λ_{II} on vertex angle 2β is presented in Fig. 2.3.

To determine parameters λ_{I} and λ_{II} from data from Tables 2.1 and 2.2, the fitting expressions had been chosen as follows [203]:

$$\lambda_{\mathrm{I}} \approx 1.247\cos\beta - 1.312\cos^2\beta + 0.8532\cos^3\beta - 0.2882\cos^4\beta, \quad 0 \le \beta \le \pi/2; \tag{2.14}$$

Table 2.1 Values of stress singularity exponent λ_{I} at the tip of elastic wedge under symmetrical loading

2β	0°	10°	15°	30°	45°	60°	75°
λ_{I}	0.5000	0.5000	0.4998	0.4986	0.4950	0.4878	0.4753
2β	90°	105°	120°	135°	150°	165°	180°
λ_{I}	0.4555	0.4261	0.3843	0.3264	0.2480	0.1427	0.0000

Table 2.2 Values of stress singularity exponent λ_{II} at the tip of elastic wedge under antisymmetrical loading

2β	0°	15°	30°	45°	60°	75°	90°	$102,5^\circ$
λ_{II}	0.5000	0.4547	0.4018	0.3403	0.2691	0.1868	0.0915	0.0000

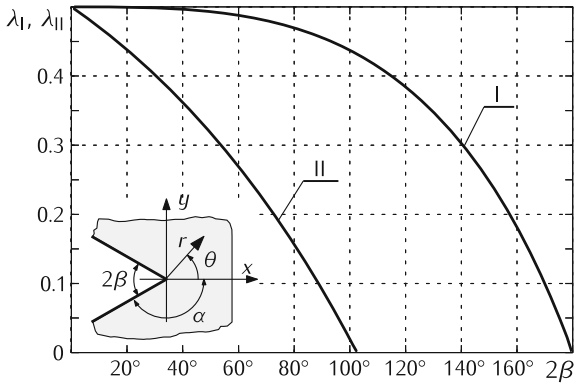

Fig. 2.3 Stress singularity exponents in the tip of V-notch λ_I (*curve* I) and λ_{II} (*curve* II) with respect to vertex angle 2β

$$\lambda_{II} \approx 0.5 - 0.3134\tan\beta - 0.2479\tan^2\beta + 0.1937\tan^3\beta - 0.0410\tan^4\beta, \quad 0 \le \beta \le \beta^*. \quad (2.15)$$

Maximal absolute error of these functions was below 0.001. They can serve as a good initial approximation for numerical solution of Eqs. (2.11) and (2.12) using Newton method.

Note that values $\lambda = 0$ obey both characteristic equations (2.11) and (2.12) at any angle values α, but this root is extraneous and generates no eigenfunctions. This root has a definite physical sense only in limit cases, when $\alpha \to \pi/2$ (symmetrical distribution) or $\alpha \to \pi - \beta^*$ (antisymmetrical distribution), see Fig. 2.3.

2.2.2 *Stress Intensity Factors in V-Notch Tip*

Hereinafter we shall consider only elastic wedges with reentrant angles, i.e., vertex angle $2\beta < \pi$, when stresses in wedge tip has a power singularity. Let us find from system (2.7) the relation between coefficients A and B

$$B = \frac{(1-\lambda)\sin(2\lambda\alpha)}{\sin(2\alpha(1-\lambda))}A = \mp\frac{\sin(2\lambda\alpha)}{\sin(2\alpha)}A, \quad (2.16)$$

where upper and lower signs correspond to symmetrical and antisymmetrical distributions, respectively.

Taking into account that at the symmetry axis (wedge bisecting line) stresses $\sigma_{\theta\theta}(r, 0)$ and $\tau_{r\theta}(r, 0)$ correspond to symmetrical and antisymmetrical parts of stress field, respectively, we get from relationships (2.4) and (2.6)

$$\sigma_{\theta\theta}(r,0)+\mathrm{i}\tau_{r\theta}(r,0)=r^{-\lambda_{\mathrm{I}}}\frac{(2-\lambda_{\mathrm{I}})\sin 2\alpha-\sin(2\lambda_{\mathrm{I}}\alpha)}{\sin 2\alpha}\,\mathrm{Re}\,A+$$
$$+\,\mathrm{i}r^{-\lambda_{\mathrm{II}}}\frac{\sin(2\lambda_{\mathrm{II}}\alpha)-\lambda_{\mathrm{II}}\sin 2\alpha}{\sin 2\alpha}\mathrm{Im}\,A. \tag{2.17}$$

Hereinafter we shall suppose that the constants A and B correspond to eigenvalues λ_{I} and λ_{II} responsible for singular stresses in the wedge tip.

Let us introduce stress intensity factors in the V-notch tip for symmetrical $\tilde{K}_{\mathrm{I}}^{\mathrm{V}}$ (mode I) and antisymmetrical $\tilde{K}_{\mathrm{II}}^{\mathrm{V}}$ (mode II) stress distributions with the following definitions [45, 214]

$$\tilde{K}_{\mathrm{I}}^{V}=\lim_{r\to 0}\left[(2\pi r)^{\lambda_{\mathrm{I}}}\sigma_{\theta\theta}(r,0)\right], \tag{2.18}$$
$$\tilde{K}_{\mathrm{II}}^{V}=\lim_{r\to 0}\left[(2\pi r)^{\lambda_{\mathrm{II}}}\tau_{r\theta}(r,0)\right]. \tag{2.19}$$

It should be noted that the alternative stress intensity factor definitions are often met in the literature as well [15, 85, 208]

$$K_{\mathrm{I}}^{\mathrm{V}}=\sqrt{2\pi}\,\lim_{r\to 0}\left[r^{\lambda_{\mathrm{I}}}\sigma_{\theta\theta}(r,0)\right], \tag{2.20}$$
$$K_{\mathrm{II}}^{\mathrm{V}}=\sqrt{2\pi}\,\lim_{r\to 0}\left[r^{\lambda_{\mathrm{II}}}\tau_{r\theta}(r,0)\right]. \tag{2.21}$$

Interrelations between these definitions are obvious

$$K_{\mathrm{I}}^{\mathrm{V}}=(2\pi)^{1/2-\lambda_{\mathrm{I}}}\,\tilde{K}_{\mathrm{I}}^{\mathrm{V}},\qquad K_{\mathrm{II}}^{\mathrm{V}}=(2\pi)^{1/2-\lambda_{\mathrm{II}}}\,\tilde{K}_{\mathrm{II}}^{\mathrm{V}}. \tag{2.22}$$

We shall apply both stress intensity factors definitions in further outline with the aim of easier comparing results of different authors.

Notice that SIF $\tilde{K}_{\mathrm{II}}^{\mathrm{V}}$ can be expressed also from polar stress gradient in the notch tip using formula

$$\tilde{K}_{\mathrm{II}}^{\mathrm{V}}=-\lim_{r\to 0}\left[\frac{(2\pi r)^{\lambda_{\mathrm{II}}}}{2-\lambda_{\mathrm{II}}}\,\frac{\partial\sigma_{\theta\theta}\,(r,0)}{\partial\theta}\right]. \tag{2.23}$$

Applying formulae (2.18) and (2.19), we obtain

$$\tilde{K}_{\mathrm{I}}^{\mathrm{V}}=(2\pi)^{\lambda_{\mathrm{I}}}\,\frac{(2-\lambda_{\mathrm{I}})\sin 2\alpha-\sin(2\lambda_{\mathrm{I}}\alpha)}{\sin 2\alpha}\mathrm{Re}\,A, \tag{2.24}$$
$$\tilde{K}_{\mathrm{II}}^{\mathrm{V}}=(2\pi)^{\lambda_{\mathrm{II}}}\,\frac{\sin(2\lambda_{\mathrm{II}}\alpha)-\lambda_{\mathrm{II}}\sin(2\alpha)}{\sin 2\alpha}\mathrm{Im}\,A. \tag{2.25}$$

From here one gets

$$\operatorname{Re} A = -\frac{\tilde{K}_{\mathrm{I}}^{\mathrm{V}}}{(2\pi)^{\lambda_{\mathrm{I}}}} \frac{\sin 2\alpha}{(\lambda_{\mathrm{I}} - 2)\sin 2\alpha + \sin(2\lambda_{\mathrm{I}}\alpha)}, \tag{2.26}$$

$$\operatorname{Im} A = \frac{\tilde{K}_{\mathrm{II}}^{\mathrm{V}}}{(2\pi)^{\lambda_{\mathrm{II}}}} \frac{\sin 2\alpha}{\sin(2\lambda_{\mathrm{II}}\alpha) - \lambda_{\mathrm{II}} \sin 2\alpha}. \tag{2.27}$$

From relationship (2.16), the constant B can be found as

$$\operatorname{Re} B = \frac{\tilde{K}_{\mathrm{I}}^{\mathrm{V}}}{(2\pi)^{\lambda_{\mathrm{I}}}} \frac{\sin(2\lambda_{\mathrm{I}}\alpha)}{(\lambda_{\mathrm{I}} - 2)\sin 2\alpha + \sin(2\lambda_{\mathrm{I}}\alpha)} \tag{2.28}$$

$$\operatorname{Im} B = \frac{\tilde{K}_{\mathrm{II}}^{\mathrm{V}}}{(2\pi)^{\lambda_{\mathrm{II}}}} \frac{\sin(2\lambda_{\mathrm{II}}\alpha)}{\sin(2\lambda_{\mathrm{II}}\alpha) - \lambda_{\mathrm{II}} \sin 2\alpha} \tag{2.29}$$

Thus, complex potentials transform into the following form [15]:

$$\begin{aligned} \Phi(z) &= -\frac{\tilde{K}_{\mathrm{I}}^{\mathrm{V}}}{(2\pi z)^{\lambda_{\mathrm{I}}}} \frac{\sin 2\alpha}{(\lambda_{\mathrm{I}} - 2)\sin 2\alpha + \sin 2\lambda_{\mathrm{I}}\alpha} \\ &\quad + \frac{\mathrm{i}\tilde{K}_{\mathrm{II}}^{\mathrm{V}}}{(2\pi z)^{\lambda_{\mathrm{II}}}} \frac{\sin 2\alpha}{\sin 2\lambda_{\mathrm{II}}\alpha - \lambda_{\mathrm{II}} \sin 2\alpha}, \\ \Psi(z) &= \frac{\tilde{K}_{\mathrm{I}}^{\mathrm{V}}}{(2\pi z)^{\lambda_{\mathrm{I}}}} \frac{\sin(2\lambda_{\mathrm{I}}\alpha)}{(\lambda_{\mathrm{I}} - 2)\sin 2\alpha + \sin 2\lambda_{\mathrm{I}}\alpha} \\ &\quad + \frac{\mathrm{i}\tilde{K}_{\mathrm{II}}^{\mathrm{V}}}{(2\pi z)^{\lambda_{\mathrm{II}}}} \frac{\sin 2\lambda_{\mathrm{II}}\alpha}{\sin 2\lambda_{\mathrm{II}}\alpha - \lambda_{\mathrm{II}} \sin 2\alpha}. \end{aligned} \tag{2.30}$$

Relationships (2.30) present solution to homogeneous singular boundary value problem of elasticity theory [45] for wedge with vertex angle $2\alpha > \pi$ in a complex stress state. This eigensolution has a clear physical meaning — it determines singular stress distribution in the wedge. Arbitrary constants $\tilde{K}_{\mathrm{I,II}}^{\mathrm{V}}$ represent stress intensity factors in the wedge tip. Relations (2.30) can serve as asymptotic at infinity during solving various homogeneous singular boundary value problems for V-shaped regions.

Substituting potentials (2.30) into relationship (2.3), we get stress tensor components in the wedge in polar coordinate system [218, 222]

$$\begin{aligned} \sigma_{rr} = {} & \frac{\tilde{K}_{\mathrm{I}}^{\mathrm{V}}}{(2\pi r)^{\lambda_{\mathrm{I}}}\, \Delta_1} \left[\frac{2 + \lambda_{\mathrm{I}}}{2 - \lambda_{\mathrm{I}}} \cos(2 - \lambda_{\mathrm{I}})\,\alpha \;\cos\lambda_{\mathrm{I}}\theta + \cos\lambda_{\mathrm{I}}\alpha \;\cos(2 - \lambda_{\mathrm{I}})\,\theta \right] + \\ & + \frac{\tilde{K}_{\mathrm{II}}^{\mathrm{V}}}{(2\pi r)^{\lambda_{\mathrm{II}}}\, \Delta_2} \left[(1 + \lambda_{\mathrm{II}}) \sin\lambda_{\mathrm{II}}\alpha \;\sin(2 - \lambda_{\mathrm{II}})\,\theta + \right. \\ & \left. + (2 + \lambda_{\mathrm{II}}) \sin(2 - \lambda_{\mathrm{II}})\,\alpha \;\sin\lambda_{\mathrm{II}}\theta \right], \end{aligned}$$

$$\sigma_{\theta\theta} = \frac{\tilde{K}_{\mathrm{I}}^{\mathrm{V}}}{(2\pi r)^{\lambda_{\mathrm{I}}}\,\Delta_1}\left[\cos(2-\lambda_{\mathrm{I}})\,\alpha\ \cos\lambda_{\mathrm{I}}\theta\ -\cos\lambda_{\mathrm{I}}\alpha\ \cos(2-\lambda_{\mathrm{I}})\,\theta\right]+$$
$$+\ \frac{\tilde{K}_{\mathrm{II}}^{\mathrm{V}}}{(2\pi r)^{\lambda_{\mathrm{II}}}\,\Delta_2}\left[(\lambda_{\mathrm{II}}-2)\sin\lambda_{\mathrm{II}}\alpha\ \sin(2-\lambda_{\mathrm{II}})\,\theta\ +\right.$$
$$\left.+\,(2-\lambda_{\mathrm{II}})\sin(2-\lambda_{\mathrm{II}})\,\alpha\ \sin\lambda_{\mathrm{II}}\theta\right],$$
$$\tau_{r\theta} = \frac{\tilde{K}_{\mathrm{I}}^{\mathrm{V}}}{(2\pi r)^{\lambda_{\mathrm{I}}}\,\Delta_1}\left[\frac{\lambda_{\mathrm{I}}}{2-\lambda_{\mathrm{I}}}\cos(2-\lambda_{\mathrm{I}})\,\alpha\ \sin\lambda_{\mathrm{I}}\theta\ -\cos\lambda_{\mathrm{I}}\alpha\ \sin(2-\lambda_{\mathrm{I}})\,\theta\right]+$$
$$+\ \frac{\tilde{K}_{\mathrm{II}}^{\mathrm{V}}}{(2\pi r)^{\lambda_{\mathrm{II}}}\,\Delta_2}\left[(2-\lambda_{\mathrm{II}})\sin\lambda_{\mathrm{II}}\alpha\ \cos(2-\lambda_{\mathrm{II}})\,\theta\ +\right.$$
$$\left.-\lambda_{\mathrm{II}}\sin(2-\lambda_{\mathrm{II}})\,\alpha\ \cos\lambda_{\mathrm{II}}\theta\right], \tag{2.31}$$

where

$$\Delta_1 = \cos(2-\lambda_{\mathrm{I}})\alpha - \cos\lambda_{\mathrm{I}}\alpha,$$
$$\Delta_2 = (2-\lambda_{\mathrm{II}})\sin\lambda_{\mathrm{II}}\alpha - \lambda_{\mathrm{II}}\sin(2-\lambda_{\mathrm{II}})\alpha.$$

Correspondingly, components of displacement vector in wedge can be represented in the form

$$u_r = \frac{\tilde{K}_{\mathrm{I}}^{\mathrm{V}} r\,(2\pi r)^{-\lambda_{\mathrm{I}}}}{2G(1-\lambda_{\mathrm{I}})\Delta_1}\left[\frac{\kappa-1+\lambda_{\mathrm{I}}}{2-\lambda_{\mathrm{I}}}\cos(2-\lambda_{\mathrm{I}})\alpha\ \cos\lambda_{\mathrm{I}}\theta\ +\cos\lambda_{\mathrm{I}}\alpha\cos(2-\lambda_{\mathrm{I}})\theta\right]+$$
$$+\ \frac{\tilde{K}_{\mathrm{II}}^{\mathrm{V}} r\,(2\pi r)^{-\lambda_{\mathrm{II}}}}{2G(1-\lambda_{\mathrm{II}})\Delta_2}\left[(2-\lambda_{\mathrm{II}})\sin\lambda_{\mathrm{II}}\alpha\ \sin(2-\lambda_{\mathrm{II}})\,\theta\ +\right.$$
$$\left.+\,(\kappa-1+\lambda_{\mathrm{II}})\sin(2-\lambda_{\mathrm{II}})\,\alpha\ \sin\lambda_{\mathrm{II}}\theta\right],$$
$$u_\theta = -\frac{\tilde{K}_{\mathrm{I}}^{\mathrm{V}} r\,(2\pi r)^{-\lambda_{\mathrm{I}}}}{2G(1-\lambda_{\mathrm{I}})\Delta_1}\left[\frac{\kappa+1-\lambda_{\mathrm{I}}}{2-\lambda_{\mathrm{I}}}\cos(2-\lambda_{\mathrm{I}})\,\alpha\ \sin\lambda_{\mathrm{I}}\theta\ +\right.$$
$$\left.+\cos\lambda_{\mathrm{I}}\alpha\ \sin(2-\lambda_{\mathrm{I}})\,\theta\right]+$$
$$+\ \frac{\tilde{K}_{\mathrm{II}}^{\mathrm{V}} r\,(2\pi r)^{-\lambda_{\mathrm{II}}}}{2G(1-\lambda_{\mathrm{II}})\Delta_2}\Big[(2-\lambda_{\mathrm{II}})\sin\lambda_{\mathrm{II}}\alpha\ \cos(2-\lambda_{\mathrm{II}})\,\theta\ +$$
$$+\,(\kappa+1-\lambda_{\mathrm{II}})\sin(2-\lambda_{\mathrm{II}})\,\alpha\ \cos\lambda_{\mathrm{II}}\theta\Big], \tag{2.32}$$

where κ is an elastic constant (see (1.18)).

Similar relations for Cartesian stress tensor components and components of displacement vector are derivable using potentials (2.30) and relationships from (1.16) to (1.18) [208]. Relationships (2.31) and (2.32) show that stress intensity factors at the tip of sharp V-notch $\tilde{K}_{\mathrm{I}}^{\mathrm{V}}$ and $\tilde{K}_{\mathrm{II}}^{\mathrm{V}}$ determine stress–strain state around the notch tip. They depend on applied loads and shape of elastic body. These parameters are therefore the main parameters of linear fracture mechanics for bodies with V-notches.

Note that relations (2.31) and (2.32) are valid only for vertex angles $2\beta < \pi$, antisymmetrical part with intensity factor $\tilde{K}_{\mathrm{II}}^{\mathrm{V}}$ being absent in the interval $\beta^* < \beta < 2\pi$

since the characteristic equation (2.12) have no solutions here. Let us consider in more detail a borderline case when $\beta \to \beta^*$ ($\lambda_{\text{II}} \to 0$). In this case complex potentials for antisymmetrical part of stress distribution

$$\begin{aligned}
\Phi_0(z) &= \mathrm{i}C + \frac{\theta \sin 2\alpha^*}{2\alpha^* - \sin 2\alpha^*} \tilde{K}_{\text{II}}^{\text{V}}, \\
z\Phi_0'(z) &= -\frac{\mathrm{i} \sin 2\alpha^*}{2\alpha^* - \sin 2\alpha^*} \tilde{K}_{\text{II}}^{\text{V}}, \\
\Psi_0(z) &= \frac{2\mathrm{i}\alpha^*}{2\alpha^* - \sin 2\alpha^*} \tilde{K}_{\text{II}}^{\text{V}}, \qquad \alpha^* = \pi - \beta^*
\end{aligned} \tag{2.33}$$

and corresponding stresses in the wedge

$$\begin{aligned}
\sigma_{rr} &= \frac{\alpha^* \sin 2\theta + 2\theta \sin 2\alpha^*}{2\alpha^* - \sin 2\alpha^*} \tilde{K}_{\text{II}}^{\text{V}}, \\
\sigma_{\theta\theta} &= \frac{2\theta \sin 2\alpha^* - 2\alpha^* \sin 2\theta}{2\alpha^* - \sin 2\alpha^*} \tilde{K}_{\text{II}}^{\text{V}}, \\
\tau_{r\theta} &= \frac{2\alpha^* \cos 2\theta - \sin 2\alpha^*}{2\alpha^* - \sin 2\alpha^*} \tilde{K}_{\text{II}}^{\text{V}}
\end{aligned} \tag{2.34}$$

are independent of radial coordinate r and depend only on the angle θ. Here C is a real constant irrelevant of stress state in the wedge. Shear stresses at wedge bisecting line are constant, i.e., $\tau_{r\theta}(r, 0) = \tilde{K}_{\text{II}}^{\text{V}}$.

This section contains results of studying stress and displacement distributions around a V-shaped notch in isotropic homogeneous linearly elastic material. Similar studies were conducted also for other materials in both linear and nonlinear approach. In particular, one can find publications devoted to studying stress distribution around V-shaped notch in viscoelastic solids [5, 24], linearly elastic orthotropic [18, 19, 78, 146, 155, 245, 247] or anisotropic materials [3, 4, 14, 17, 22, 49–51, 61, 95, 101, 102, 104, 130, 169, 246]. Publications are also known on piecewise homogeneous wedge consisting of isotropic [8, 9, 20, 21, 23, 34, 35, 40, 41, 59, 60, 62, 66, 86, 91, 100, 118–122, 137, 139, 151, 152, 154, 159, 175–177, 179, 183–185, 223, 228, 233], orthotropic [248, 249], or anisotropic [52–54, 97, 103, 117, 131, 138, 148, 250] materials. Several works present stress state around V-shaped notch in nonlinear homogeneous [38, 39, 74, 124–127, 134, 145, 160, 237, 241, 252, 253, 260, 261, 267] or piecewise homogeneous [209, 265] materials.

It should be highlighted that the knowledge about stress–strain state distribution near V-shaped notch gives as a foundation for experimental techniques for notch stress intensity factor determination [87].

2.2.3 Constructing General Solution Using Eigenfunctions

Characteristic equations (2.11) and (2.12) have an infinite number of roots, some of them possibly being complex. Corresponding to these roots eigensolutions (eigenvalues) in form of complex potentials, stresses, or displacements obey zero boundary conditions for stresses at wedge faces. General solution to plane elasticity theory problem for region with sharp V-notch can be written in the form of eigenfunction series with unknown constant coefficients. Such approach had been used in many applications, for example, in finite element method at simulating a special element with sharp V-notch [7, 57, 70, 140, 217–220, 235, 254, 255] and boundary collocations method for finite elastic bodies with V-notches. In such cases unknown coefficients are sought from equations system obtained by obeying boundary conditions in points of collocation at elastic region's boundary beyond the notch faces [29–33, 85, 163].

Based on relationships (2.31) and (2.32), which are valid for other eigenvalues as well, the general solution can be rewritten also in terms of stresses and displacements as

$$\begin{aligned}
\sigma_{ij}(r,\theta) &= \sum_{n=0}^{\infty}\left[\sigma_{ij,s}^{(n)}(r,\theta,\lambda_{\mathrm{I}}^{(n)}) + \sigma_{ij,a}^{(n)}(r,\theta,\lambda_{\mathrm{II}}^{(n)})\right],\\
\sigma_{r\theta}(r,\theta) &= \tau_{r\theta}(r,\theta),\\
u_i(r,\theta) &= \sum_{n=0}^{\infty}\left[u_{i,s}^{(n)}(r,\theta,\lambda_{\mathrm{I}}^{(n)}) + u_{i,a}^{(n)}(r,\theta,\lambda_{\mathrm{II}}^{(n)})\right], \qquad i,j = r,\theta, \qquad (2.35)
\end{aligned}$$

where symmetrical

$$\begin{aligned}
\sigma_{rr,s}^{(n)} &= \frac{A_n}{r^{\lambda_{\mathrm{I}}^{(n)}}\Delta_1^{(n)}}\left[\frac{2+\lambda_{\mathrm{I}}^{(n)}}{2-\lambda_{\mathrm{I}}^{(n)}}\cos(2-\lambda_{\mathrm{I}}^{(n)})\alpha\ \cos\lambda_{\mathrm{I}}^{(n)}\theta + cos\lambda_{\mathrm{I}}^{(n)}\alpha\ \cos(2-\lambda_{\mathrm{I}}^{(n)})\theta\right],\\
\sigma_{\theta\theta,s}^{(n)} &= \frac{A_n}{r^{\lambda_{\mathrm{I}}^{(n)}}\Delta_1^{(n)}}\left[\cos(2-\lambda_{\mathrm{I}}^{(n)})\alpha\ \cos\lambda_{\mathrm{I}}^{(n)}\theta - \cos\lambda_{\mathrm{I}}^{(n)}\alpha\ \cos(2-\lambda_{\mathrm{I}}^{(n)})\theta\right],\\
\sigma_{r\theta,s}^{(n)} &= \frac{A_n}{r^{\lambda_{\mathrm{I}}^{(n)}}\Delta_1^{(n)}}\left[\frac{\lambda_{\mathrm{I}}^{(n)}}{2-\lambda_{\mathrm{I}}^{(n)}}\cos(2-\lambda_{\mathrm{I}}^{(n)})\alpha\ \sin\lambda_{\mathrm{I}}^{(n)}\theta - \cos\lambda_{\mathrm{I}}^{(n)}\alpha\ \sin(2-\lambda_{\mathrm{I}}^{(n)})\theta\right];\\
u_{r,s}^{(n)} &= \frac{A_n r^{1-\lambda_{\mathrm{I}}^{(n)}}}{2G(1-\lambda_{\mathrm{I}}^{(n)})\Delta_1^{(n)}}\left[\frac{\kappa-1+\lambda_{\mathrm{I}}^{(n)}}{2-\lambda_{\mathrm{I}}^{(n)}}\cos(2-\lambda_{\mathrm{I}}^{(n)})\alpha\ \cos\lambda_{\mathrm{I}}^{(n)}\theta + \right.\\
&\qquad \left. + \cos\lambda_{\mathrm{I}}^{(n)}\alpha\ \cos(2-\lambda_{\mathrm{I}}^{(n)})\theta\right],\\
u_{\theta,s}^{(n)} &= \frac{-A_n r^{1-\lambda_{\mathrm{I}}^{(n)}}}{2G(1-\lambda_{\mathrm{I}}^{(n)})\Delta_1^{(n)}}\left[\frac{\kappa+1-\lambda_{\mathrm{I}}^{(n)}}{2-\lambda_{\mathrm{I}}^{(n)}}\cos(2-\lambda_{\mathrm{I}}^{(n)})\alpha\ \sin\lambda_{\mathrm{I}}^{(n)}\theta + \right.\\
&\qquad \left. + \cos\lambda_{\mathrm{I}}^{(n)}\alpha\ \sin(2-\lambda_{\mathrm{I}}^{(n)})\theta\right] \qquad (2.36)
\end{aligned}$$

and antisymmetrical

$$\sigma_{rr,a}^{(n)} = \frac{B_n}{r^{\lambda_{\mathrm{II}}^{(n)}} \Delta_2^{(n)}} \Big[(1+\lambda_{\mathrm{II}}^{(n)}) \sin \lambda_{\mathrm{II}}^{(n)} \alpha \ \sin(2-\lambda_{\mathrm{II}}^{(n)})\theta + \\ + (2+\lambda_{\mathrm{II}}^{(n)}) \sin(2-\lambda_{\mathrm{II}}^{(n)})\alpha \ \sin \lambda_{\mathrm{II}}^{(n)} \theta \Big],$$

$$\sigma_{\theta\theta,a}^{(n)} = \frac{B_n}{r^{\lambda_{\mathrm{II}}^{(n)}} \Delta_2^{(n)}} \Big[(\lambda_{\mathrm{II}}^{(n)}-2) \sin \lambda_{\mathrm{II}}^{(n)} \alpha \ \sin(2-\lambda_{\mathrm{II}}^{(n)})\theta + \\ + (2-\lambda_{\mathrm{II}}^{(n)}) \sin(2-\lambda_{\mathrm{II}}^{(n)})\alpha \ \sin \lambda_{\mathrm{II}}^{(n)} \theta \Big],$$

$$\sigma_{r\theta,a}^{(n)} = \frac{A_n}{r^{\lambda_{\mathrm{I}}^{(n)}} \Delta_2^{(n)}} \Big[(2-\lambda_{\mathrm{II}}^{(n)}) \sin \lambda_{\mathrm{II}}^{(n)} \alpha \ \cos(2-\lambda_{\mathrm{II}}^{(n)})\theta + \\ - \lambda_{\mathrm{II}}^{(n)} \sin(2-\lambda_{\mathrm{II}}^{(n)})\alpha \ \cos \lambda_{\mathrm{II}}^{(n)} \theta \Big];$$

$$u_{r,a}^{(n)} = \frac{B_n r^{1-\lambda_{\mathrm{II}}^{(n)}}}{2G(1-\lambda_{\mathrm{II}}^{(n)})\Delta_2^{(n)}} \Big[(2-\lambda_{\mathrm{II}}^{(n)}) \sin \lambda_{\mathrm{II}}^{(n)} \alpha \ \sin(2-\lambda_{\mathrm{II}}^{(n)})\theta + \\ + (\kappa - 1 + \lambda_{\mathrm{II}}^{(n)}) \sin(2-\lambda_{\mathrm{II}}^{(n)})\alpha \ \sin \lambda_{\mathrm{II}}^{(n)} \theta \Big],$$

$$u_{\theta,a}^{(n)} = \frac{B_n r^{1-\lambda_{\mathrm{II}}^{(n)}}}{2G(1-\lambda_{\mathrm{II}}^{(n)})\Delta_2^{(n)}} \Big[(2-\lambda_{\mathrm{II}}^{(n)}) \sin \lambda_{\mathrm{II}} \alpha \ \cos(2-\lambda_{\mathrm{II}}^{(n)})\theta + \\ + \left(\kappa + 1 - \lambda_{\mathrm{II}}^{(n)}\right) \sin(2-\lambda_{\mathrm{II}}^{(n)})\alpha \ \cos \lambda_{\mathrm{II}}^{(n)} \theta \Big] \qquad (2.37)$$

parts of eigensolutions contain arbitrary constants A_n and B_n, respectively. Here

$$\Delta_1^{(n)} = \cos(2-\lambda_{\mathrm{I}}^{(n)})\alpha - \cos \lambda_{\mathrm{I}}^{(n)} \alpha,$$
$$\Delta_2^{(n)} = (2-\lambda_{\mathrm{II}}^{(n)}) \sin \lambda_{\mathrm{II}}^{(n)} \alpha - \lambda_{\mathrm{II}}^{(n)} \sin(2-\lambda_{\mathrm{II}}^{(n)})\alpha;$$

$\lambda_{\mathrm{I}}^{(n)}$ and $\lambda_{\mathrm{II}}^{(n)}$ are roots of characteristic equations (2.11) and (2.12), where $\lambda_{\mathrm{I}}^{0} = \lambda_{\mathrm{I}}$, $\lambda_{\mathrm{I}}^{0} = \lambda_{\mathrm{II}}$; constants A_0 and B_0 are connected with stress intensity factors $\tilde{K}_{\mathrm{I}}^{\mathrm{V}}$ and $\tilde{K}_{\mathrm{II}}^{\mathrm{V}}$ by obvious interrelation.

Eigensolutions representation in the form (2.36) and (2.37) is valid, generally speaking, only for real eigenvalues $\lambda_{\mathrm{I}}^{(n)}$ and $\lambda_{\mathrm{II}}^{(n)}$. If eigenvalues are complex, formulae (2.36) and (2.37) must be modified in such way that right sides were real, because their left sides are real (see e.g. [218]). This can be made by taking into consideration the fact that each complex eigenvalue has its conjugated eigenvalue. It follows from the structure of characteristic equations (2.11) and (2.12).

Relationships (2.30) can serve as a starting point for similarly expanding the general solution in terms of complex potentials.

2.3 Semi-infinite Curvilinear Notches in Elastic Plane

2.3.1 Parabolic Notch

2.3.1.1 Symmetrical Loading

Assume that a semi-infinite crack is located in elastic plane along the negative semi-axis x. Kolosov–Muskhelishvili complex stress potentials, which determine principal initial stress state as follows from relationships (2.30), have the following form for the symmetrical loading:

$$\Phi_0(z) = \frac{K_\mathrm{I}}{2\sqrt{2\pi z}}, \qquad \Psi_0(z) = \frac{K_\mathrm{I}}{4\sqrt{2\pi z}}, \qquad z = x + \mathrm{i}y, \tag{2.38}$$

where K_I is stress intensity factor at a crack tip. In this general approach, stresses σ_y^0 at the complementary semi-axis x are given by the formula

$$\sigma_y^0(x, 0) = \frac{K_\mathrm{I}}{\sqrt{2\pi}} x^{-1/2}, \qquad (x > 0). \tag{2.39}$$

Consider now a parabolic notch with the contour L specified by equation

$$z = \frac{\rho}{2}(1 - i\eta)^2, \qquad -\infty < \eta < \infty. \tag{2.40}$$

The parabola (2.40) has focus in point $z = 0$ and vertex in point $z = \rho/2$. Here ρ is radius of curvature in notch tip (Fig. 2.4). When radius of curvature approaches zero, parabolic notch transforms into the semi-infinite crack. Assume that the principal stress state in elastic region is determined by potentials (2.38) and that notch contour L is free of stresses

$$N_*(t) + \mathrm{i}T_*(t) = 0, \qquad t \in L. \tag{2.41}$$

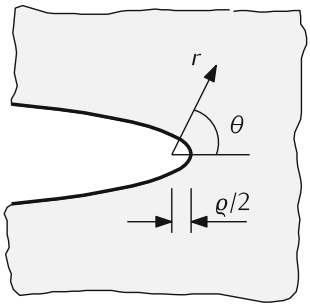

Fig. 2.4 Parabolic notch in elastic plane

where $N_*(t)$ and $T_*(t)$ are normal and shear components of stress vector at notch contour.

Complex stress potentials for plane with a parabolic notch are sought as the sum

$$\Phi_*(z) = \Phi_0(z) + \Phi(z), \qquad \Psi_*(z) = \Psi_0(z) + \Psi(z), \tag{2.42}$$

where functions $\Phi_0(z)$ and $\Psi_0(z)$ are defined by the formulae (2.38) and potentials $\Phi(z)$ and $\Psi(z)$ describe disturbed stress state induced by the notch [15]

$$\Phi(z) = 0, \qquad \Psi(z) = \frac{\rho K_{\mathrm{I}}}{2\, z\sqrt{2\pi z}}. \tag{2.43}$$

Maximal stress (in the tip of parabola) is equal to

$$(\sigma_y^*)_{\max} = \frac{2K_{\mathrm{I}}}{\sqrt{\pi\rho}} \tag{2.44}$$

Taking into account relationships (2.39), the last equality is in the form

$$(\sigma_y^*)_{\max} = \frac{K_{\mathrm{I}}}{\sqrt{2\pi}} R_{\mathrm{I}} \rho^{-1/2}, \qquad (R_{\mathrm{I}} = 2\sqrt{2}). \tag{2.45}$$

Introduced here factor R_{I} (stress rounding factor) characterizes transition from the stress σ_y^* in vicinity of sharp notch or crack tip to the maximal stress σ_y^* in the tip of rounded notch. The formula (2.44) has found a wide application in engineering practice for estimating maximal stresses in tips of narrow notches. It was first published by Irwin [98], and thereafter it is frequently encountered in later publications [6, 48, 56, 75, 81, 82, 89, 133, 156, 162, 189, 229].

From relationships (2.44) or (2.45), a formula follows to determine stress intensity factor in crack tip through stress concentration factor or maximal stress $\sigma_{\max}$ in the tip of narrow notch [36, 98, 181, 189, 225]

$$K_{\mathrm{I}} = \lim_{\rho \to 0} \left(\sqrt{\pi\rho}\, \frac{\sigma_{\max}}{2} \right). \tag{2.46}$$

It should be highlighted that the formula (2.46) has not general applicability. It is valid only at transition from a parabolic notch or a notch reducible to parabolic (for example, hyperbolic notch with zero vertex angle) to crack. Such transition depends not only on radius of curvature ρ, but also factor R_{I}, which in its turn depends on notch shape in vicinity of its tip.

Based on precise solution to the problem about elastic plane with elliptical hole under tension, the limit transition with major axis of an ellipse approaching infinity was used to construct formulae for symmetrical stress distribution near parabolic notch tip [56]

$$\sigma_x = \frac{K_\mathrm{I}}{\sqrt{2\pi r}}\left[\cos\frac{\theta}{2}\left(1-\sin\frac{\theta}{2}\ \sin\frac{3\theta}{2}\right)-\frac{\rho}{2r}\cos\frac{3\theta}{2}\right],$$
$$\sigma_y = \frac{K_\mathrm{I}}{\sqrt{2\pi r}}\left[\cos\frac{\theta}{2}\left(1+\sin\frac{\theta}{2}\ \sin\frac{3\theta}{2}\right)+\frac{\rho}{2r}\cos\frac{3\theta}{2}\right],$$
$$\tau_{xy} = \frac{K_\mathrm{I}}{\sqrt{2\pi r}}\left[\sin\frac{\theta}{2}\cos\frac{\theta}{2}\ \cos\frac{3\theta}{2}-\frac{\rho}{2r}\sin\frac{3\theta}{2}\right], \tag{2.47}$$

where r, θ, ($z = x + \mathrm{i}y = r\exp(\mathrm{i}\theta)$) are polar coordinates with pole in focus of parabola (see Fig. 2.4).

Using formulae (2.42) and (2.43), we obtain corresponding relations for displacement components [164]

$$2Gu = K_\mathrm{I}\sqrt{\frac{r}{2\pi}}\left[\left(\kappa-\frac{1}{2}\right)\cos\frac{\theta}{2}-\frac{1}{2}\cos\frac{3\theta}{2}+\frac{\rho}{r}\cos\frac{\theta}{2}\right],$$
$$2Gv = K_\mathrm{I}\sqrt{\frac{r}{2\pi}}\left[\left(\kappa+\frac{1}{2}\right)\sin\frac{\theta}{2}-\frac{1}{2}\sin\frac{3\theta}{2}+\frac{\rho}{r}\sin\frac{\theta}{2}\right], \tag{2.48}$$

where designations are the same as used for crack (1.64).

Note that formulae (2.47) ensue also directly from complex stress potentials (2.42) and (2.43) derived for the parabolic notch. These formulae frequently find application as asymptotic expressions at estimating stress distribution near narrow notches with small relative rounding radius in the tip.

2.3.1.2 Antisymmetrical Loading

Complex stress potentials for semi-infinite crack along the negative semi-axis, which determine principal initial stress state as follows from relationships (2.30), have the following form for the antisymmetrical loading

$$\Phi_0(z) = -\frac{\mathrm{i}K_\mathrm{II}}{2\sqrt{2\pi z}}, \qquad \Psi_0(z) = \frac{3\mathrm{i}K_\mathrm{II}}{4\sqrt{2\pi z}}, \qquad z = x + \mathrm{i}y, \tag{2.49}$$

where K_II is stress intensity factor at a crack tip. In this general approach, stresses τ^0_{xy} at the complementary semi-axis x are given by the formula

$$\tau^0_{xy}(x,0) = \frac{K_\mathrm{II}}{\sqrt{2\pi}}x^{-1/2} \qquad (x > 0). \tag{2.50}$$

Again complex stress potentials for elastic plane with a parabolic notch are sought as the sum (2.42), where principal stress state is determined by potentials (2.49) while disturbed stress state induced by the parabolic notch is described by functions [15]

$$\Phi(z) = 0, \qquad \Psi(z) = -\frac{\mathrm{i}\rho K_{\mathrm{II}}}{2z\sqrt{2\pi z}}. \tag{2.51}$$

This time normal and shear components of stress vector at notch tip are zero. Shear stresses reach maximum values in the point that lays inside the elastic region on axis Ox at the distance ρ from parabola tip

$$\tau_{\max} = \tau^*_{xy}\left(\frac{3\rho}{2},\ 0\right) = \frac{2K_{\mathrm{II}}}{3\sqrt{3\pi\rho}}. \tag{2.52}$$

Extremal values of tangential normal stress at the notch contour are attained in points $x = 0, y = \pm\rho$

$$\sigma^*_{s,\mathrm{extr}} = \mp\frac{K_{\mathrm{II}}}{\sqrt{\pi\rho}} \tag{2.53}$$

Taking into account relationships (2.50), write the last equality in the form

$$\left|\sigma^*_{s,\mathrm{extr}}\right| = \frac{K_{\mathrm{II}}}{\sqrt{2\pi}} R_{\mathrm{II}}\, \rho^{-1/2}, \qquad (R_{\mathrm{II}} = \sqrt{2}), \tag{2.54}$$

where stress rounding factor R_{II} plays under antisymmetrical loading the same role as the factor R_{I} under symmetrical loading.

From relationship (2.53), a formula follows to determine stress intensity factor in crack tip K_{II} through stress concentration factor or maximal stress $\sigma_{\max}$ near the tip of narrow notch under antisymmetrical loading [189, 225]

$$K_{\mathrm{II}} = \lim_{\rho\to 0}\left(\sqrt{\pi\rho}\sigma_{\max}\right). \tag{2.55}$$

Corresponding formula connecting the factor K_{II} and maximal shear stresses $\tau_{\max}$ can be derived based on the relation (2.52) [15, 178, 189, 266]

$$K_{\mathrm{II}} = \lim_{\rho\to 0}\left(\frac{3}{2}\sqrt{3\pi\rho}\tau_{\max}\right). \tag{2.56}$$

The formulae (2.55) and (2.56) are valid only at transition from a parabolic notch or a notch reducible to parabolic to crack. It must be noted that the relation (2.56) in some publications is erroneously presented [36, 181] in somewhat another form.

Based on the precise solution to the problem about elastic plane with elliptical hole under tension, the formulae were constructed for antisymmetrical stress distribution near parabolic notch tip as well [56]

$$\sigma_x = -\frac{K_{\mathrm{II}}}{\sqrt{2\pi r}}\left[\sin\frac{\theta}{2}\left(2 + \cos\frac{\theta}{2}\ \cos\frac{3\theta}{2}\right) - \frac{\rho}{2r}\sin\frac{3\theta}{2}\right],$$
$$\sigma_y = \frac{K_{\mathrm{II}}}{\sqrt{2\pi r}}\left[\sin\frac{\theta}{2}\ \cos\frac{\theta}{2}\ \cos\frac{3\theta}{2} - \frac{\rho}{2r}\sin\frac{3\theta}{2}\right],$$

$$\tau_{xy} = \frac{K_{\mathrm{II}}}{\sqrt{2\pi r}}\left[\cos\frac{\theta}{2}\left(1-\sin\frac{\theta}{2}\,\sin\frac{3\theta}{2}\right)-\frac{\rho}{2r}\,\cos\frac{3\theta}{2}\right]. \tag{2.57}$$

Using formulae (2.42) and (2.51), we obtain corresponding relations for displacement components [164]

$$\begin{aligned} 2Gu &= K_{\mathrm{II}}\sqrt{\frac{r}{2\pi}}\left[\left(\kappa+\frac{3}{2}\right)\sin\frac{\theta}{2}+\frac{1}{2}\cos\frac{3\theta}{2}-\frac{\rho}{r}\sin\frac{\theta}{2}\right],\\ 2Gv &= K_{\mathrm{II}}\sqrt{\frac{r}{2\pi}}\left[\left(-\kappa+\frac{3}{2}\right)\cos\frac{\theta}{2}-\frac{1}{2}\cos\frac{3\theta}{2}+\frac{\rho}{r}\cos\frac{\theta}{2}\right], \end{aligned} \tag{2.58}$$

where designations are the same as used for crack (1.64).

Note that formulae (2.57) are also in accordance with the analytical solution (2.42), (2.49) and (2.51). The relationships (2.44), (2.52) and (2.53) can be readily derived asymptotically [189] for small relative radius of curvature in the tip of elliptical hole, if precise problem solution is known. General solution to homogeneous boundary value problem for elastic plane with a parabolic notch had been derived also by Cherepanov [45] in somewhat another form than relationships (2.42), (2.43) and (2.51).

2.3.1.3 Complex-Stressed State

In the case of complex loading, stress distribution around tip of a parabolic notch will be described by expressions that can be obtained as sums of relationships (2.47) and (2.57). The same expressions in polar coordinate system r, θ are [164]

$$\begin{aligned} \begin{Bmatrix}\sigma_r\\ \sigma_\theta\\ \tau_{r\theta}\end{Bmatrix} &= \frac{1}{4}\frac{K_{\mathrm{I}}}{\sqrt{2\pi r}}\begin{Bmatrix}5\cos\frac{\theta}{2}-\cos\frac{3}{2}\theta-\frac{2\rho}{r}\cos\frac{\theta}{2}\\ 3\cos\frac{\theta}{2}+\cos\frac{3}{2}\theta+\frac{2\rho}{r}\cos\frac{\theta}{2}\\ \sin\frac{\theta}{2}+\sin\frac{3}{2}\theta+\frac{2\rho}{r}\sin\frac{\theta}{2}\end{Bmatrix}+\\ &+\frac{1}{4}\frac{K_{\mathrm{II}}}{\sqrt{2\pi r}}\begin{Bmatrix}-5\sin\frac{\theta}{2}+3\sin\frac{3}{2}\theta-\frac{2\rho}{r}\sin\frac{\theta}{2}\\ -\sin\frac{\theta}{2}-\sin\frac{3}{2}\theta+\frac{2\rho}{r}\sin\frac{\theta}{2}\\ \cos\frac{\theta}{2}+3\cos\frac{3}{2}\theta-\frac{2\rho}{r}\cos\frac{\theta}{2}\end{Bmatrix}. \end{aligned} \tag{2.59}$$

Corresponding formulae for displacements have the form

$$\begin{aligned} \begin{Bmatrix}2Gu_r\\ 2Gu_\theta\end{Bmatrix} &= K_{\mathrm{I}}\sqrt{\frac{r}{2\pi}}\begin{Bmatrix}\left(\kappa-\frac{1}{2}\right)\cos\frac{\theta}{2}-\frac{1}{2}\cos\frac{3}{2}\theta+\frac{\rho}{r}\cos\frac{1}{2}\theta\\ -\left(\kappa+\frac{1}{2}\right)\sin\frac{\theta}{2}+\frac{1}{2}\sin\frac{3}{2}\theta-\frac{\rho}{r}\sin\frac{1}{2}\theta\end{Bmatrix}+\\ &+K_{\mathrm{II}}\sqrt{\frac{r}{2\pi}}\begin{Bmatrix}-\left(\kappa-\frac{1}{2}\right)\sin\frac{\theta}{2}+\frac{3}{2}\sin\frac{3}{2}\theta+\frac{\rho}{r}\sin\frac{\theta}{2}\\ -\left(\kappa+\frac{1}{2}\right)\cos\frac{\theta}{2}+\frac{3}{2}\cos\frac{3}{2}\theta+\frac{\rho}{r}\cos\frac{\theta}{2}\end{Bmatrix}. \end{aligned} \tag{2.60}$$

To estimate limit equilibrium of bodies with sharp or rounded notches under complex stress state, there is a concept of elastic strain energy density in fracture mechanics [167, 170, 224]. Strain energy density in polar coordinate system can be represented as

$$W = \frac{1}{2}\left[\sigma_r \frac{\partial u_r}{\partial r} + \sigma_\theta \left(\frac{u_r}{r} + \frac{1}{r}\frac{\partial u_\theta}{\partial \theta}\right) + \tau_{r\theta}\left(\frac{1}{r}\frac{\partial u_r}{\partial \theta} + \frac{\partial u_\theta}{\partial r} - \frac{u_\theta}{r}\right)\right]. \tag{2.61}$$

Substituting components of stresses (2.59) and displacements (2.60), one comes to [164]

$$W = \frac{1}{r}\left(a_{11}K_{\mathrm{I}}^2 + 2a_{12}K_{\mathrm{I}}K_{\mathrm{II}} + a_{22}K_{\mathrm{II}}^2\right), \tag{2.62}$$

where

$$\begin{aligned}
a_{11} &= \frac{1}{8G}\left[(1+\cos\theta)(\kappa - \cos\theta) + \left(\frac{\rho}{r}\right)^2\right],\\
a_{12} &= \frac{1}{8G}\left\{[2\cos\theta - (\kappa - 1)]\sin\theta - \frac{2\rho}{r}\sin\theta\right\},\\
a_{22} &= \frac{1}{8G}\left\{[\kappa(1-\cos\theta) + (1+3\cos\theta)\cos\theta] - \frac{4\rho}{r}\cos\theta + \left(\frac{\rho}{r}\right)^2\right\}.
\end{aligned} \tag{2.63}$$

At $\rho = 0$, the expression (2.62) transforms into well-known relationship [167, 170] for strain energy density in mechanics of cracks.

2.3.2 *Hyperbolic Notch*

2.3.2.1 Symmetrical Loading

Let us consider elastic wedge with the tip in coordinate system origin and vertex angle 2α ($\pi/2 < \alpha < \pi$) (Fig. 2.5). Wedge edges are located in left half-plane and described by equation

$$y = \pm x \tan\alpha. \tag{2.64}$$

Kolosov–Muskhelishvili complex stress potentials, which determine principal stress state have the following form for the symmetrical loading (see (2.30)):

$$\begin{aligned}
\Phi_0^s(z) &= -\frac{K_{\mathrm{I}}^{\mathrm{V}}}{\sqrt{2\pi}}\frac{\sin 2\alpha}{(\lambda_{\mathrm{I}} - 2)\sin 2\alpha + \sin 2\lambda_{\mathrm{I}}\alpha}\, z^{-\lambda_{\mathrm{I}}},\\
\Psi_0^s(z) &= \frac{K_{\mathrm{I}}^{\mathrm{V}}}{\sqrt{2\pi}}\frac{\sin(2\lambda_{\mathrm{I}}\alpha)}{(\lambda_{\mathrm{I}} - 2)\sin 2\alpha + \sin 2\lambda_{\mathrm{I}}\alpha}\, z^{-\lambda_{\mathrm{I}}},
\end{aligned} \tag{2.65}$$

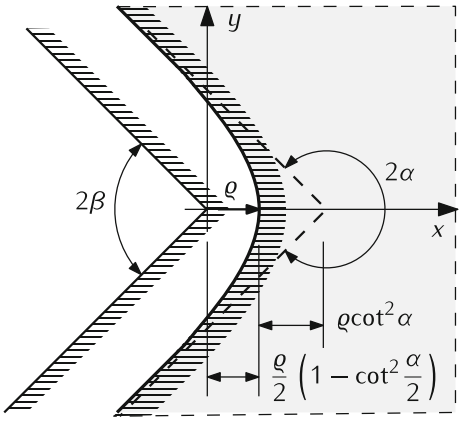

Fig. 2.5 Hyperbolic notch in elastic plane

where $K_{\mathrm{I}}^{\mathrm{V}}$ is notch stress intensity factor in the wedge tip introduced so as stresses σ_y^0 at the complementary semi-axis x are determined by the formula

$$\sigma_y^0(x,0) = \frac{K_{\mathrm{I}}^{\mathrm{V}}}{\sqrt{2\pi}}\, x^{-\lambda_{\mathrm{I}}} \qquad (x > 0). \tag{2.66}$$

Let the hyperbolic notch be cut in the elastic wedge so that the notch's contour L (namely, left branch of hyperbola) is described by the equation [15]

$$z = \rho \frac{\cos\alpha}{\cos\alpha - \cos(\xi\alpha)} \exp(-\mathrm{i}\xi\alpha), \qquad -1 < \xi < 1. \tag{2.67}$$

Asymptotes to the hyperbola

$$y = \pm x \tan\alpha \pm \frac{\rho}{\sin\alpha} \tag{2.68}$$

intersect with angle 2β ($0 \le \beta = \pi - \alpha < \pi/2$), its focus is located in point $z = 0$, and its vertex in point

$$z = \rho \frac{\cos\alpha}{\cos\alpha - 1} = \frac{\rho}{2}\left(1 - \cot^2\frac{\alpha}{2}\right).$$

Radius of hyperbola curvature in its vertex equals to ρ. At $\alpha = \pi$, hyperbola converges into parabola (2.40).

The problem for disturbed stress state induced in the wedge by a hyperbolic notch with unloaded contour L was reduced [15] to Sherman–Lauricella integral equation [153], which can be solved numerically. The results of stress rounding factor R_{I} in the formula for maximal stresses in notch tip

Table 2.3 Stress rounding factor R_{I} for different vertex angles of hyperbolic notch

2β	R_I			
	Benthem [15]	Lazzarin–Tovo [133]	Strandberg [229]	Filippi et al. [75]
0°	$2\sqrt{2}$	$2\sqrt{2}$	—	$2\sqrt{2}$
30°	2.814	2.912	3.01	3.013
60°	2.769	2.906	3.03	3.080
90°	2.665	2.768	2.98	2.985
120°	2.444	2.460	2.81	2.675
150°	1.992	1.946	2.24	2.087
165°	1.613	1.576	—	—
180°	1	1	—	—

$$\left(\sigma_y^*\right)_{\max} = \frac{K_{\mathrm{I}}^{\mathrm{V}}}{\sqrt{2\pi}} R_{\mathrm{I}} \rho^{-\lambda_{\mathrm{I}}} \tag{2.69}$$

are presented in Table 2.3.

2.3.2.2 Antisymmetrical Loading

Complex stress potentials in this case are similarly sought in the form (2.42), where principal stress state in accordance with relationships (2.30) is given by functions

$$\begin{aligned} \Phi_0^a(z) &= \frac{\mathrm{i}K_{\mathrm{II}}^{\mathrm{V}}}{\sqrt{2\pi}} \frac{\sin 2\alpha}{\sin 2\lambda_{\mathrm{II}}\alpha - \lambda_{\mathrm{II}} \sin 2\alpha} z^{-\lambda_{\mathrm{II}}}, \\ \Psi_0^a(z) &= \frac{\mathrm{i}K_{\mathrm{II}}^{\mathrm{V}}}{\sqrt{2\pi}} \frac{\sin 2\lambda_{\mathrm{II}}\alpha}{\sin 2\lambda_{\mathrm{II}}\alpha - \lambda_{\mathrm{II}} \sin 2\alpha} z^{-\lambda_{\mathrm{II}}}, \end{aligned} \tag{2.70}$$

where $K_{\mathrm{II}}^{\mathrm{V}}$ is notch stress intensity factor in the wedge tip and stresses τ_{xy}^0 at the complementary semi-axis x are determined by the formula

$$\tau_{xy}^0(x, 0) = \frac{K_{\mathrm{II}}^{\mathrm{V}}}{\sqrt{2\pi}} x^{-\lambda_{\mathrm{II}}} \qquad (x > 0). \tag{2.71}$$

Extremal normal stresses are attained in two points of the notch contour and can be represented as [15]

$$\left|\sigma_{s,\mathrm{extr}}^*\right| = \frac{K_{\mathrm{II}}^{\mathrm{V}}}{\sqrt{2\pi}} R_{\mathrm{II}} \rho^{-\lambda_{\mathrm{II}}}, \tag{2.72}$$

where numerical values of the factor R_{II} are given in Table 2.4. The table presents also coordinates of extremum points (coordinate x' has origin in the vertex of hyperbola)

Table 2.4 Values of parameter λ_{II}, factor R_{II}, and coordinate of points, in which normal stress is equal to $\pm\left|\sigma_{s,\text{extr}}\right|$ [15]

2α	λ_{II}	R_{II}	x'/ρ	$\mp y/\rho$
257.4534°	0	1.666844	−0.669	1.426
260°	0.019525	1.674068	−0.581	1.281
270°	0.091471	1.715070	−0.469	1.076
300°	0.269099	1.803234	−0.446	0.979
330°	0.401808	1.7567	−0.480	0.988
360°	0.5	$\sqrt{2}$	−0.5	1

Table 2.5 Values of parameter λ_{II}, maximal dimensionless shear stress $\tilde{\tau}_{\max} = \sqrt{2\pi}\,\rho^{\lambda_{II}}\tau_{\max}/K_{II}^{V}$ and coordinates of points at axis x, in which the maximum is attained [15]

2α	λ_{II}	$\tilde{\tau}_{\max}$	x'/ρ
257.4534°	0	1	∞
260°	0.019525	0.954819	5.83
270°	0.091471	0.877002	2.184
300°	0.269099	0.776696	1.208
330°	0.401808	0.695245	1.038
360°	0.5	$2\sqrt{2}/(3\sqrt{3})$	1

$$x - x' = \frac{\rho}{2}\left(1 - \cot^2\frac{\alpha}{2}\right).$$

Maximal shear stresses $\tau_{\max}$ are attained in inner points at the axis x. Their coordinates x' and dimensionless values of stress are presented in Table 2.5.

2.3.3 Curvilinear Notch of Special Shape

2.3.3.1 Approach of Lazarin and Tovo [133]

Lazarin and Tovo [133] were first who had derived stress distribution around the curvilinear notch tip, which can be approximated by a rounded V-notch with vertex angle 2β (Fig. 2.6). To construct the solution to this problem, they have used curvilinear coordinates u and v, which are binded with Cartesian coordinates x and y by relationship

$$z = x + \mathrm{i}y = w^q = (u + \mathrm{i}v)^q, \qquad q = 2\,(1 - \beta/\pi)\,. \tag{2.73}$$

The line $u = 0$ in new coordinate system is an image of wedge boundary with vertex angle $2\alpha = 2(\pi - \beta)$. Coordinate curve $u = u_0 = r_0^{1/q}$, where r_0 is the distance

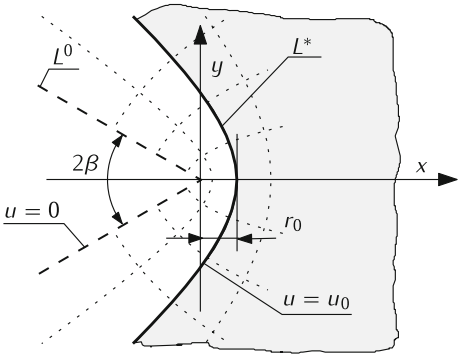

Fig. 2.6 Curvilinear notch of special shape

of its vertex from origin of coordinate system, corresponds to edge of curvilinear semi-infinite notch (Fig. 2.6). Radius of curvature in the notch tip ρ depends on the distance r_0: $\rho = qr_0/(q-1)$. Selecting different distances r_0, it is possible to obtain curvilinear notches with different curvatures in their tips.

Then the approximate eigensolutions for thus defined curvilinear semi-infinite notches in elastic plane has been found. On this basis, approximate expressions binding stress components in elastic region to notch stress intensity factors $K_{\mathrm{I}}^{\mathrm{V}}$ and $K_{\mathrm{II}}^{\mathrm{V}}$ in the tip of respective sharp V-notch were written as follows

$$\begin{Bmatrix} \sigma_{\theta\theta} \\ \sigma_{rr} \\ \tau_{r\theta} \end{Bmatrix} = \frac{1}{\sqrt{2\pi}} \frac{r^{-\lambda_{\mathrm{I}}} K_{\mathrm{I}}^{\mathrm{V}}}{2-\lambda_{\mathrm{I}}+\chi_{\mathrm{I}}\lambda_{\mathrm{I}}} \left[\begin{Bmatrix} (2-\lambda_{\mathrm{I}})\cos\lambda_{\mathrm{I}}\theta \\ (2+\lambda_{\mathrm{I}})\cos\lambda_{\mathrm{I}}\theta \\ \lambda_{\mathrm{I}}\sin\lambda_{\mathrm{I}}\theta \end{Bmatrix} + \right.$$
$$+\chi_{\mathrm{I}}\lambda_{\mathrm{I}} \begin{Bmatrix} \cos(2-\lambda_{\mathrm{I}})\theta \\ -\cos(2-\lambda_{\mathrm{I}})\theta \\ \sin(2-\lambda_{\mathrm{I}})\theta \end{Bmatrix} +$$
$$\left. + \left(\frac{r}{r_0}\right)^{\mu_{\mathrm{I}}+\lambda_{\mathrm{I}}-1} (2+\lambda_{\mathrm{I}}-\chi_{\mathrm{I}}\lambda_{\mathrm{I}}) \begin{Bmatrix} \cos(1+\mu_{\mathrm{I}})\theta \\ -\cos(1+\mu_{\mathrm{I}})\theta \\ \sin(1+\mu_{\mathrm{I}})\theta \end{Bmatrix} \right] +$$
$$+ \frac{1}{\sqrt{2\pi}} \frac{r^{-\lambda_{\mathrm{II}}} K_{\mathrm{II}}^{\mathrm{V}}}{\lambda_{\mathrm{II}}+\chi_{\mathrm{II}}(2-\lambda_{\mathrm{II}})} \left[\begin{Bmatrix} -(2-\lambda_{\mathrm{II}})\sin\lambda_{\mathrm{II}}\theta \\ -(2+\lambda_{\mathrm{II}})\sin\lambda_{\mathrm{II}}\theta \\ \lambda_{\mathrm{II}}\cos\lambda_{\mathrm{II}}\theta \end{Bmatrix} + \right.$$
$$+\chi_{\mathrm{II}}(2-\lambda_{\mathrm{II}}) \begin{Bmatrix} -\sin(2-\lambda_{\mathrm{II}})\theta \\ \sin(2-\lambda_{\mathrm{II}})\theta \\ \cos(2-\lambda_{\mathrm{II}})\theta \end{Bmatrix} +$$
$$\left. + \left(\frac{r}{r_0}\right)^{\mu_{\mathrm{II}}+\lambda_{\mathrm{II}}-1} [\lambda_{\mathrm{II}}-\chi_{\mathrm{II}}(2-\lambda_{\mathrm{II}})] \begin{Bmatrix} \sin(1+\mu_{\mathrm{II}})\theta \\ -\sin(1+\mu_{\mathrm{II}})\theta \\ -\cos(1+\mu_{\mathrm{II}})\theta \end{Bmatrix} \right], \tag{2.74}$$

where r, θ are polar coordinates with pole in V-notch tip ($z = r\exp(\mathrm{i}\theta)$); $\lambda_\mathrm{I}, \lambda_\mathrm{II} \in (0, 1)$ are roots of characteristic equations (2.11) and (2.12);

$$\begin{aligned}
\chi_\mathrm{I} &= -\sin\frac{\lambda_\mathrm{I} q\pi}{2}\sin^{-1}\frac{(2-\lambda_\mathrm{I})q\pi}{2},\\
\chi_\mathrm{II} &= -\sin\frac{\lambda_\mathrm{II} q\pi}{2}\sin^{-1}\frac{(2-\lambda_\mathrm{II})q\pi}{2},\\
\mu_\mathrm{I} &= \frac{1}{q} - \frac{\lambda_\mathrm{I}^2 - (2-\lambda_\mathrm{I})/q + \chi_\mathrm{I}\lambda_\mathrm{I}(2-\lambda_\mathrm{I}-1/q)}{2+\lambda_\mathrm{I}-\chi_\mathrm{I}\lambda_\mathrm{I}} - 1,\\
\mu_\mathrm{II} &= -\frac{(2+\lambda_\mathrm{II})\lambda_\mathrm{II} - \chi_\mathrm{II}(2-\lambda_\mathrm{II})^2}{\lambda_\mathrm{II}-\chi_\mathrm{II}(2-\lambda_\mathrm{II})} - 1.
\end{aligned} \tag{2.75}$$

Starting from these expressions for the case of symmetrical loading, the analytical dependence of maximal stresses $\sigma_{\max} = (\sigma_y)_{\max}$ in the notch tip on stress intensity factor K_I^V, vertex angle of V-notch 2β, and radius of curvature in the notch tip ρ, has been found

$$\sigma_{\max} = \frac{4K_\mathrm{I}^\mathrm{V}\rho^{-\lambda_\mathrm{I}}}{\sqrt{2\pi}\left[(2-\lambda_\mathrm{I}) - \lambda_\mathrm{I}\dfrac{\sin(\lambda_\mathrm{I}\alpha)}{\sin\alpha\,(2-\lambda_\mathrm{I})}\right]\left(\dfrac{\pi-2\beta}{2\alpha}\right)^{\lambda_\mathrm{I}}}. \tag{2.76}$$

Comparison of this relation (2.76) with solutions to specific problems for specimens with rounded V-notches had revealed poor accuracy of derived formula. Therefore, later [75] the solution (2.76) was revised to improve accuracy. As a result, formula that is much more complicated was obtained

$$\sigma_{\max} = \frac{K_\mathrm{I}^\mathrm{V}}{\sqrt{2\pi}}(1+\tilde{\omega}_1)\left(\frac{\pi-2\beta}{2\alpha}\rho\right)^{-\lambda_\mathrm{I}} \tag{2.77}$$

where

$$\begin{aligned}
\tilde{\omega}_1 &= \frac{(1+\mu)\chi_d + \chi_c}{(2-\lambda)+\lambda\chi_b}\frac{\alpha}{2(\pi-2\beta)},\\
\chi_b &= -\frac{\sin\lambda_\mathrm{I}\alpha}{\sin(2-\lambda_\mathrm{I})\alpha},\\
\chi_c &= \left[(1-\mu)^2 - (1+\mu)/q\right]\left[2+\lambda_\mathrm{I}(1-\gamma_b)\right] - (3-\mu)\varepsilon,\\
\chi_d &= (1/q-1-\mu)\left[2+\lambda_\mathrm{I}(1-\gamma_b)\right] - \varepsilon,\\
\varepsilon &= \lambda_\mathrm{I}^2 + \lambda_\mathrm{I}(2-\lambda)\chi_b - (2-\lambda_\mathrm{I})/q - \lambda,
\end{aligned} \tag{2.78}$$

and μ ($\mu < \lambda_\mathrm{I}$) is the root of equation

$$\chi_d(1+\mu)\cos(1-\mu)\alpha + \chi_c\cos(1+\mu)\alpha = 0.$$

Note that if in formulae (2.76) and (2.77) we put $\alpha = \pi$, we get relationship (2.44), i.e., we return thereby to a parabolic notch. Numerical results for the factor R_{I} in relationship (2.69) calculated using these formulae are presented in Table 2.3, maximal stress data (2.77) being calculated only for those notch vertex angles, for which values of parameters μ, χ_b, χ_c and χ_d are known [75]. There was introduced a concept of generalized stress intensity factors for rounded notches in the same publication. Later these matters were considered in more details in papers [63–65, 83, 94, 132, 136, 144].

The generalized stress intensity factor for the case of symmetrical loading when maximal normal stress $\sigma_{\max}$ is attained in notch tip can be presented in the form [132]

$$K^{\mathrm{V}}_{\rho,\mathrm{I}} = \sigma_{\max} \frac{\sqrt{2\pi}}{1+\tilde{\omega}_1} \left(\frac{q-1}{q} \rho \right)^{\lambda_1}. \tag{2.79}$$

When the angle $\beta = 0$, ($q = 2$, $\lambda_1 = 1/2$, $\tilde{\omega}_1 = 1$), an equality follows from the formula (2.79)

$$K^{\mathrm{V}}_{\rho,\mathrm{I}} = \frac{1}{2} \sigma_{\max} \sqrt{\pi \rho}, \tag{2.80}$$

which coincides with relationship (2.44) for the parabolic notch, if the following substitution is made therein: $K^{\mathrm{V}}_{\mathrm{I}} = K^{\mathrm{V}}_{\rho,\mathrm{I}}$. The same conclusion is valid for relationship (2.77) for a general notch type.

Similar relationships were also introduced for antisymmetrical loading [132] in terms of maximal shear stresses attained in inner points of elastic region at the wedge bisecting line.

2.3.3.2 Rounded Notch in the Edge of Half-Plane

Interrelation between stress concentration and stress intensity factors was studied also for the rounded boundary notch in half-plane [229]. In this case, the tip of sharp V-notch with vertex angle 2β was rounded along the circular arc with radius ρ and length $2\rho\varphi$ ($\varphi = \pi/2 - \beta$). The circular arc was smoothly connected with straight edges of sharp notch using third order (cubic) curves (Fig. 2.7). If the rounding radius is small in comparison with notch depth, we come to semi-infinite rounded notch (principle of microscope [45]).

The problem of stress concentration in elastic half-plane with thus constructed smooth curvilinear notch was reduced to Sherman–Lauricella integral equation [153], which was solved by a numerical technique. In order to derive the relationship (2.69) independent on configuration of elastic region beyond the V-notch, sufficiently small curvature radius values of the notch tip in comparison with the notch's depth were examined. Table 2.3 demonstrates values of factor R_{I} calculated for five angles β. Strandberg [229] failed to find numerical solution in above outlined way for the angle $\beta = 0$; nevertheless, he mentioned that such solution is already known and it is met with the result (2.45) for a parabolic notch.

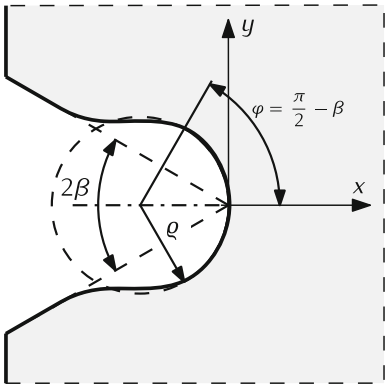

Fig. 2.7 Edge rounded notch in half-plane

Analysis of data in Table 2.3 shows that values of dimensionless factor R_{I} obtained by various authors converge only for angles $\beta = 0$ (parabolic notch) and $\beta = \pi/2$ (smooth edge). For other angle β values, relative difference between published data is as high as 10 %. The relationship (2.69) that contains the factor R_{I} is frequently applied in engineering calculations, in particular, for approximate stress concentration factor estimations in tip of rounded V-notch with small radius of curvature based on known stress intensity factor in tip of corresponding sharp V-notch. It can be also used to find stress intensity factors starting from solution to the problem concerning stress concentration near rounded notches. Therefore, it is desirable to have values of factor R_{I} with accuracy as high as possible.

Discrepancies in data presented above as well as lack of solution for most important shape of rounded V-notch, that is for wedge with rectilinear faces and tip rounded by the circular arc, stimulated the present authors to conduct their own study of this problem [192].

2.4 Rounded V-Notch Under Symmetrical Loading

2.4.1 Problem Definition and Reduction to Singular Integral Equation [192]

2.4.1.1 Problem statement

Let the elastic plane contain sharp V-notch with the tip in coordinate system origin and vertex angle 2β, $(0 \leq \beta < \pi)$ (Fig. 2.8a). Assume that stress state of the notched plane is determined by complex potentials $\Phi_0^s(z)$ and $\Psi_0^s(z)$ (2.65) presented in somewhat different form

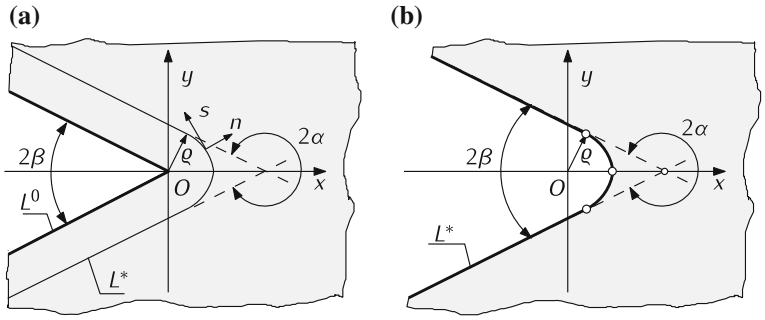

Fig. 2.8 Sharp (**a**) and rounded (**b**) V-notches

$$\Phi_0^s(z) = -\frac{\tilde{K}_{\mathrm{I}}^{\mathrm{V}}}{(2\pi)^{\lambda_{\mathrm{I}}}} \frac{\sin 2\alpha}{(\lambda_{\mathrm{I}} - 2)\sin 2\alpha + \sin 2\lambda_{\mathrm{I}}\alpha} z^{-\lambda_{\mathrm{I}}},$$
$$\Psi_0^s(z) = \frac{\tilde{K}_{\mathrm{I}}^{\mathrm{V}}}{(2\pi)^{\lambda_{\mathrm{I}}}} \frac{\sin(2\lambda_{\mathrm{I}}\alpha)}{(\lambda_{\mathrm{I}} - 2)\sin 2\alpha + \sin 2\lambda_{\mathrm{I}}\alpha} z^{-\lambda_{\mathrm{I}}}, \tag{2.81}$$

which ensure zero stresses at the notch contour L^0.

Let us consider the smooth contour L^* composing of straight segments parallel to wedge faces L^0 and circular arc with radius ρ in its tip. Let us write the vector of normal (σ_n^0) and shear (τ_{ns}^0) stresses at this contour

$$\sigma_n^0 + \mathrm{i}\tau_{ns}^0 = \Phi_0^s(t) + \overline{\Phi_0^s(t)} + \frac{\mathrm{d}\bar{t}}{\mathrm{d}t}\left[t\overline{\Phi_0'^s(t)} + \overline{\Psi_0^s(t)}\right] = -p(t), \qquad t \in L^*. \tag{2.82}$$

Now consider the rounded V-notch with the same vertex angle and free of stresses contour L^* in the plane (Fig. 2.8b). Let an asymptotic stress distribution be given at infinity, which is determined by potentials $\Phi_0^s(z)$ and $\Psi_0^s(z)$ (2.65). We shall apply a superposition technique to solve this boundary value problem. Write above stress potentials in the form

$$\Phi_*(z) = \Phi_0^s(z) + \Phi(z), \qquad \Psi_*(z) = \Psi_0^s(z) + \Psi(z), \tag{2.83}$$

where $\Phi(z)$ and $\Psi(z)$ are Kolosov–Muskhelishvili functions describing the disturbed stress state induced by a rounded V-notch L^*.

To find the disturbed stress state, we have to solve the boundary value problem for elastic plane containing the rounded V-notch with a contour L^*, at which the boundary condition

$$\sigma_n + \mathrm{i}\tau_{ns} = p(t), \qquad t \in L^*, \tag{2.84}$$

is satisfied, and stresses vanish at infinity.

Since stresses vanish at infinity, the disturbed stress state can be obtained also as a limit case of plane with smooth symmetrical curvilinear crack L along the contour

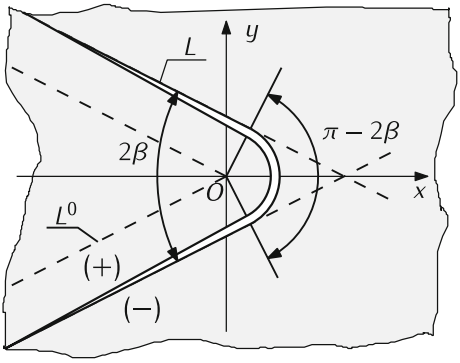

Fig. 2.9 Curvilinear crack along contour of rounded V-notch

L^* (Fig. 2.9) by elongating it to infinity and loading its edges with stresses

$$\sigma_n^+ + \mathrm{i}\tau_{ns}^+ = \sigma_n^- + \mathrm{i}\tau_{ns}^- = p\,(t)\,, \qquad t \in L, \tag{2.85}$$

where upper indexes indicate limit values of respective parameters at contour L when approaching it from the left $(+)$ or from the right $(-)$. It was the last method we applied to solve the above-stated problem.

2.4.1.2 Singular Integral Equation of the Problem

The problem for stress distribution in elastic plane with a curvilinear crack will be solved here using the method of singular integral equations [188]. Integral representation of the solution is taken in the form

$$\begin{aligned} \Phi\,(z) &= \frac{1}{2\pi}\int\limits_L \frac{g'(t)}{t-z}\,\mathrm{d}t, \\ \Psi\,(z) &= \frac{1}{2\pi}\int\limits_L \left[\frac{\overline{g'(t)}}{t-z}\,\mathrm{d}\bar{t} - \frac{\bar{t}g'(t)}{(t-z)^2}\,\mathrm{d}t\right]. \end{aligned} \tag{2.86}$$

Using expressions of stress field components $\sigma_x, \sigma_y, \tau_{xy}$ in terms of complex potentials $\Phi(z)$ and $\Psi(z)$ (1.16) and (1.17), and satisfying the boundary conditions (2.85), we get the singular integral equation of the problem [188]

$$\frac{1}{\pi}\int\limits_L \left[K\left(t,t'\right)\,g'\,(t)\,\mathrm{d}t + L\left(t,t'\right)\overline{g'\,(t)}\,\mathrm{d}\bar{t}\right] = p\left(t'\right), \qquad t' \in L, \tag{2.87}$$

with kernels $K\left(t,t'\right)$ and $L\left(t,t'\right)$ being given by formulae (1.59).

A unique solution of integral equation (2.87) in class of functions, which have an integrable singularity at the ends of integration contours exists, if the additional condition is satisfied

$$\int_L g'(t)\,\mathrm{d}t = 0, \tag{2.88}$$

which ensures uniqueness of displacements during tracing the crack contour.

The equation of crack contour can be written in the parametric form

$$t = l\omega(\xi) = l\begin{cases} (\xi+\xi_0)\cos\beta + \varepsilon\sin\beta + \\ \qquad +\mathrm{i}\left[(\xi+\xi_0)\sin\beta - \varepsilon\cos\beta\right], & -1 \le \xi < -\xi_0, \\ \varepsilon\cos(\xi/\varepsilon) + \mathrm{i}\varepsilon\sin(\xi/\varepsilon), & -\xi_0 \le \xi \le \xi_0, \\ -(\xi-\xi_0)\cos\beta + \varepsilon\sin\beta + \\ \qquad +\mathrm{i}\left[(\xi-\xi_0)\sin\beta + \varepsilon\cos\beta\right], & \xi_0 \le \xi \le 1, \end{cases} \tag{2.89}$$

where $\xi_0 = 1/(1+\tilde{\theta})$ is the value of parameter ξ corresponding to straight-to-curvilinear transition point at the crack contour; $\tilde{\theta}$ is straight segments length to circular segment length ratio; ρ is radius of circular segment; $\varepsilon = \rho/l$. The length of crack is $2l = \rho(\pi - 2\beta)\left(1+\tilde{\theta}\right)$.

As calculations show, the same solution is obtained in the assumption that the crack contour L is infinite and coincides with notch contour L^* ($L = L^*$). Such approach greatly simplifies solution of the problem since there is no need in limit transition between contours. In this approach, equation of notch/crack contour can be written in the parametric form

$$t = \rho\omega(\xi), \qquad \omega(\xi) = \mathrm{e}^{I\xi\alpha}\begin{cases} -1/\sin(\xi\alpha-\beta), & -1 < \xi < -\xi_B, \\ 1, & -\xi_B \le \xi \le \xi_B, \\ 1/\sin(\xi\alpha+\beta), & \xi_B < \xi < 1, \end{cases} \tag{2.90}$$

where $\xi_B = (\pi/2 - \beta)/\alpha$ is dimensionless angular coordinate of a contour point L, in which the circular arc transforms into the straight segment.

Let us examine in parallel the similar problem for the hyperbolic notch that was solved earlier [15] using the method of Sherman–Lauricella integral equations (see also Sect. 2.2.2). Parametric equation for this problem has the form

$$t = \rho\omega(\xi), \qquad \omega(\xi) = \frac{\mathrm{e}^{-\mathrm{i}\xi\alpha}\cos\alpha}{\cos\alpha - \cos\xi\alpha} + \frac{1}{2}\cot^2\frac{\alpha}{2} + \frac{1}{2}, \quad \alpha = \pi - \beta, \quad -1 < \xi < 1. \tag{2.91}$$

Vortices of both notches lay in the point $z = \rho$ (Fig. 2.10).

Based on parametric equations (2.90) and (2.91), reduce the Eqs. (2.87) and (2.88) to the dimensionless form

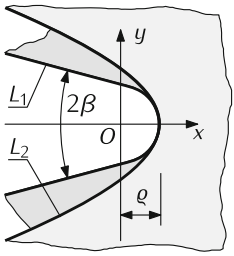

Fig. 2.10 Comparison of two contours L_1 (rounded V-notch) and L_2 (hyperbolic notch) with identical vertex angles $2\beta = \pi/6$ and notch tip rounding radii ρ

$$\begin{cases} \dfrac{1}{\pi}\displaystyle\int_{-1}^{1}\left[M\left(\xi,\eta\right)u\left(\xi\right)+N\left(\xi,\eta\right)\overline{u\left(\xi\right)}\right]\dfrac{\mathrm{d}\xi}{\sqrt{1-\xi^2}}=p\left(\eta\right), \\ \displaystyle\int_{-1}^{1}u\left(\xi\right)\dfrac{\mathrm{d}\xi}{\sqrt{1-\xi^2}}=0, \end{cases} \tag{2.92}$$

where

$$\begin{aligned} t' &= \rho\omega\left(\eta\right), \\ M\left(\xi,\eta\right) &= \rho K\left(\rho\omega\left(\xi\right),\rho\omega\left(\eta\right)\right), \\ N\left(\xi,\eta\right) &= \rho L\left(\rho\omega\left(\xi\right),\rho\omega\left(\eta\right)\right), \\ \frac{u\left(\xi\right)}{\sqrt{1-\xi^2}} &= \frac{1}{p}g'\left(\rho\omega\left(\xi\right)\right)\omega'\left(\xi\right), \\ p(\eta) &= \frac{1}{p}p(\rho\omega(\eta)), \qquad p=\tilde{K}_1^{\mathrm{V}}/(2\pi\rho)^{\lambda_1}. \end{aligned} \tag{2.93}$$

Make the substitution to increase the accuracy of integral equation (2.92) solution as recommended in [67, 68, 99]

$$\xi = G\left(\tau\right) = a\sinh\left(\mu\tau\right), \qquad \mu = \operatorname{arsinh}\frac{1}{a}, \quad \eta = G\left(\zeta\right), \tag{2.94}$$

which maps a interval $\tau \in [-1, 1]$ onto the interval $\xi \in [-1, 1]$. Such nonlinear transformation produces thickening of quadrature nodes near the point $\xi = 0$. The constant a in the substitution (2.94) is chosen based on numerical experiments (here we adopted $a = 10^{-5}$).

Now Eq. (2.92) transforms into the following

$$\begin{cases} \dfrac{1}{\pi}\displaystyle\int_{-1}^{1}\left[M\left(\xi,\eta\right)u^*\left(\tau\right)+N\left(\xi,\eta\right)\overline{u^*\left(\tau\right)}\right]\dfrac{\mathrm{d}\tau}{\sqrt{1-\tau^2}}=p\left(\eta\right), \\ \displaystyle\int_{-1}^{1}u^*\left(\tau\right)\dfrac{\mathrm{d}\tau}{\sqrt{1-\tau^2}}=0, \end{cases} \tag{2.95}$$

where the following designation was introduced

$$\frac{u^*(\tau)}{\sqrt{1-\tau^2}} = \frac{u(\xi)\,G'(\tau)}{\sqrt{1-\xi^2}}. \tag{2.96}$$

Solve the Eq. (2.95) numerically using quadrature method and applying Gauss–Chebyshev quadratures (1.100) and (1.101) to compute integrals. The system of linear complex algebraic equations $2n$ will result

$$\begin{cases} \dfrac{1}{2n}\displaystyle\sum_{k=1}^{2n}\left[M\left(\xi_k,\eta_m\right)u^*\left(\tau_k\right)+N\left(\xi_k,\eta_m\right)\overline{u^*\left(\tau_k\right)}\right]=p\left(\eta_m\right), \\ \qquad\qquad\qquad\qquad\qquad\qquad\qquad\qquad m=1,\ldots,(2n-1), \\ \dfrac{1}{2n}\displaystyle\sum_{k=1}^{2n}u^*\left(\tau_k\right)=0, \end{cases} \tag{2.97}$$

where

$$\xi_k = G\left(\tau_k\right), \qquad \tau_k = \cos\frac{\pi\,(2k-1)}{4n}, \quad k=1,\ldots,2n; \tag{2.98}$$

$$\eta_m = G\left(\zeta_m\right), \qquad \zeta_m = \cos\frac{\pi m}{2n}, \quad m=1,\ldots,2n-1. \tag{2.99}$$

The problem is symmetrical with respect to axis x, thereby providing satisfaction of symmetry condition [208]

$$u^*(-\tau) = \overline{u^*(\tau)}. \tag{2.100}$$

Taking into account relationship (2.100), one can twice reduce order of the system (2.97). As a result, we come to the following system of algebraic equations:

$$\begin{cases} \dfrac{1}{2n}\displaystyle\sum_{k=1}^{n}\left[M^*\left(\xi_k,\eta_m\right)u^*\left(\tau_k\right)+N^*\left(\xi_k,\eta_m\right)\overline{u^*\left(\tau_k\right)}\right]=p\left(\eta_m\right), \\ \qquad\qquad\qquad\qquad\qquad\qquad\qquad\qquad m=1,\ldots,n, \\ \dfrac{1}{2n}\displaystyle\sum_{k=1}^{2n}\left[u^*(\tau_k)+\overline{u^*(\tau_k)}\right]=0, \end{cases} \tag{2.101}$$

where

$$\begin{aligned} M^*\left(\xi_k,\eta_m\right) &= M\left(\xi_k,\eta_m\right)+N\left(-\xi_k,\eta_m\right), \\ N^*\left(\xi_k,\eta_m\right) &= N\left(\xi_k,\eta_m\right)+M\left(-\xi_k,\eta_m\right). \end{aligned} \tag{2.102}$$

For the collocation node $\eta_n = 0$ at the axis of symmetry (x axis), respective complex equation of the system (2.101) is reduced to real one due to symmetry

of the problem. Finally, at $m = 1, \ldots, n$, we get $2n - 1$ real equations, which create, together with the last real equation, a closed system of $2n$ real algebraic equations for n complex unknown functions $u^*(\tau_k)$, $(k = 1, 2, \ldots, n)$.

2.4.2 *Symmetrical Stress Distribution in Plane with Rounded V-Notch [192]*

2.4.2.1 Stresses at Notch Contour

Tangential normal stresses at right edge of crack/notch L (at contour of rounded V-notch) are derivable from the relationship

$$\sigma_s^* = 4\mathrm{Re}\,\left[\Phi_0^s(t) + \Phi^-(t)\right], \qquad t \in L, \tag{2.103}$$

which follows from (1.159) in absence of loads at notch contour.

Boundary value of potential $\Phi(z)$ at contour L is computable using Sokhotski–Plemelj formula (1.34). Considering substitutions (2.93) and (2.94) as well as first of formulae (2.65), one gets

$$\begin{aligned}\sigma_s^*(\eta) = 4\frac{\tilde{K}_{\mathrm{I}}^{\mathrm{V}}}{(2\pi\rho)^{\lambda_{\mathrm{I}}}}\,\mathrm{Re}\,\Bigg[&\frac{-\sin 2\alpha}{(\lambda_{\mathrm{I}} - 1)\sin 2\alpha + \sin 2\lambda_{\mathrm{I}}\alpha}\,\frac{1}{[\omega(\eta)]^{\lambda_{\mathrm{I}}}} + \\ &-\frac{\mathrm{i}}{2}\frac{u^*(\varsigma)}{G'(\varsigma)\omega'(\eta)\sqrt{1-\varsigma^2}} + \frac{1}{2\pi}\int_{-1}^{1}\frac{u^*(\tau)}{\omega(\xi)-\omega(\eta)}\,\frac{\mathrm{d}\tau}{\sqrt{1-\tau^2}}\Bigg] = \\ = \frac{\tilde{K}_{\mathrm{I}}^{\mathrm{V}}}{(2\pi\rho)^{\lambda_{\mathrm{I}}}}&\,R_{\mathrm{I}}(\beta,\eta).\end{aligned} \tag{2.104}$$

Apply the quadrature formula (1.100) to compute singular integral in relationship (2.104). Using the condition of symmetry (2.100), we can find dimensionless stress $R_{\mathrm{I}}(\beta, \eta_j)$ in nodes $\varsigma_j = \cos(j\pi/(2n))$, $j = 1, \ldots, (2n-1)$ from the formula

$$\begin{aligned}R_{\mathrm{I}}(\beta,\eta_j) = 4\mathrm{Re}\,\Bigg\{&\frac{-\sin 2\alpha}{(\lambda_{\mathrm{I}} - 2)\sin 2\alpha + \sin 2\lambda_{\mathrm{I}}\alpha}\,\frac{1}{(\omega(\eta_j))^{\lambda_{\mathrm{I}}}} + \\ &-\frac{\mathrm{i}}{2}\frac{u^*(\varsigma_j)}{G'(\varsigma_j)\omega'(\eta_j)\sqrt{1-\varsigma_j^2}} + \\ &+\frac{1}{4n}\sum_{k=1}^{n}\left[\frac{u^*(\tau_k)}{\omega(\xi_k)-\omega(\eta_j)} + \frac{\overline{u^*(\tau_k)}}{\overline{\omega(\xi_k)}-\omega(\eta_j)}\right]\Bigg\}.\end{aligned} \tag{2.105}$$

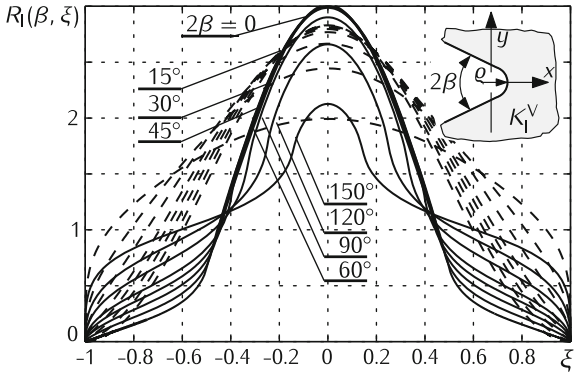

Fig. 2.11 Comparison of dimensionless stress distributions along rounded V-notch (*solid curve*) or hyperbolic notch (*dashed curve*) for various vertex angles at symmetrical loading

Values of function $u^*(\tau)$ in arbitrary point $\tau \neq \tau_k$ are computable with the help of interpolation formula (1.98). Again using the condition of symmetry (2.100), we get the following relation

$$u(\tau) = \frac{1}{2n} \sum_{k=1}^{n} (-1)^k \, T_{2n}(\tau) \sqrt{1 - \tau_k^2} \left[\frac{\overline{u(\tau_k)}}{\tau + \tau_k} - \frac{u(\tau_k)}{\tau - \tau_k} \right]. \tag{2.106}$$

Since in nodes $\varsigma_m = \cos(\pi m/(2n))$ $(m = 1, \ldots, n-1)$ Chebyshev polynomial is $T_{2n}(\varsigma_m) = (-1)^m$, we have

$$u(\varsigma_m) = \frac{1}{2n} \sum_{k=1}^{n} (-1)^{k+m} \sqrt{1 - \tau_k^2} \left[\frac{\overline{u(\tau_k)}}{\varsigma_m + \tau_k} - \frac{u(\tau_k)}{\varsigma_m - \tau_k} \right]. \tag{2.107}$$

Authors [111, 112] had calculated dimensionless stress $R_I(\beta, \xi)$ along notch contour for vertex angles $2\beta \in [0, \pi]$ and two different contour geometries L (2.90) (rounded V-notch) or (2.91) (hyperbolic notch) with identical radii of curvature in tips ρ (Fig. 2.11). We can see that stress distributions along notch contour is essentially different in these two cases. Their relative differences reach 10 % in the notch tip.

2.4.2.2 V-Notch Stress Rounding Factor

In the notch tip $z = \rho$ $(\xi = 0)$ dimensionless stress $R_I(\beta, 0)$ reaches the maximal value $R_I(\beta) = R_I$. The effect of notch tip rounding on maximal stresses is described by expression [15]

$$\left(\sigma_s^*\right)_{\max} = \frac{\tilde{K}_I^V}{(2\pi)^{\lambda_I}} R_I \rho^{-\lambda_I}. \tag{2.108}$$

The stress rounding factor in the expression is computable using formula (2.105). We can find values of functions $u^*(\tau)$ in the point $\tau = 0$ using the interpolation polynomial (2.107), which for this case has a simplified form

$$u^*(0) = \frac{1}{n}\sum_{k=1}^{n}(-1)^{k+n}\,\mathrm{Re}\;u^*(\tau_k)\tan\frac{\pi(2k-1)}{4n}. \tag{2.109}$$

Calculations of stress rounding factor values $R_\mathrm{I}(\beta)$ were performed for notch vertex angles 2β changing in the interval $0 \le 2\beta < \pi$ with increment $\pi/360$. So fine resolution was necessary to construct a sufficiently accurate fitting function $R_\mathrm{I}(\beta)$ for rounded V-notch. We had estimated the accuracy of stress rounding factor R_I determination procedure in the following way: the order of algebraic equations systems (2.101) was doubled until the relative difference R_I for the given angle β became less than 0.1 %.

For hyperbolic notch (2.91), obtained values of factor R_I were in good accordance with known results [15], the relative difference being below 0.1%, which confirmed correctness of present calculations. Figure 2.12 demonstrates dependence of the factor $R_\mathrm{I}(\beta)$ on vertex angle 2β. At $2\beta = \pi$ both curves gain the obvious value $R_\mathrm{I} = 1$. At $\beta = 0$, when the hyperbolic notch transforms into the parabolic one, the

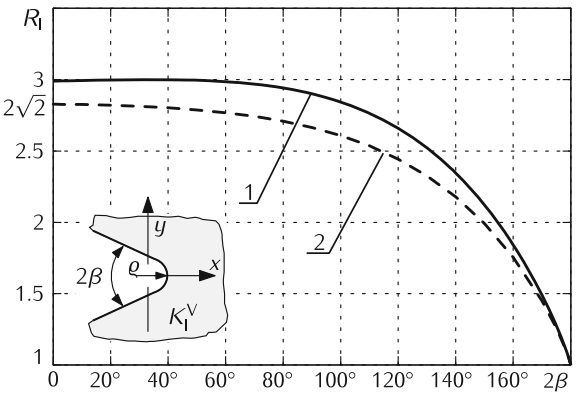

Fig. 2.12 Influence of notch geometry on factor R_I at various vertex angles 2β: rounded V-notch (1) versus hyperbolic notch (2)

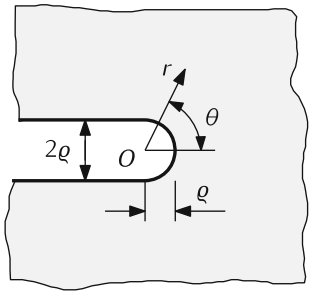

Fig. 2.13 U-notch in elastic plane

value $R_{\mathrm{I}} = 2\sqrt{2}$ is observed. At $2\beta = 0$, when the rounded V-notch transforms into a U-shaped notch (Fig. 2.13), observed value $R_{\mathrm{I}} = 2,992$ is close to known results [128, 142]. Relative differences of results for hyperbolic and rounded V-notches reaches $6 \div 10\,\%$ at vertex angles $2\beta < 2\pi/3$ that confirms the essential influence of notch geometry on maximal stresses near notch tip.

Note that maximal stresses (2.108) in the tip of U-shaped notch ($\lambda_{\mathrm{I}} = 1/2$) virtually coincide with respective values for semi-infinite crack with a circular hole of the radius ρ in its tip [47]

$$\sigma_{\max} = 2.991\,\frac{K_{\mathrm{I}}}{\sqrt{2\pi\rho}}, \tag{2.110}$$

where K_{I} is stress intensity factor at a crack tip. An asymptotic solution had been built for the last problem as well [129].

Since the stress rounding factor R_{I} for rounded V-notch will be often used in next sections, calculated values of R_{I} are presented in Table 2.6 for individual notch vertex angles.

These results were used to construct the fitting expression [203]

$$R_{\mathrm{I}} = \frac{1 + 28.75\gamma + 98.04\gamma^2 - 102.1\gamma^3 + 47.42\gamma^4 - 8.441\gamma^5}{1 + 20.71\gamma}, \quad \gamma = \pi/2 - \beta, \tag{2.111}$$

which provides relative errors less than $0.1\,\%$ in the interval $\beta \in [0^\circ,\ 83^\circ]$ and $0.4\,\%$ in the interval $\beta \in [83^\circ,\ 90^\circ]$. Coefficients at γ^4 and γ^5 in the formula (2.111) slightly differ from those published in [192, 193], that gave us a possibility to reach higher accuracy.

Above-presented analysis shows that interrelation between stress intensity and stress concentration factors for sharp and rounded notches depends not only on radius of curvature in the notch tip, but also on notch shape near the tip. In past, many researchers had believed that the relation (2.44) is precise for narrow U-shaped notches ($\beta = 0$), that is the difference between parabolic and U-shaped notches was neglected (see, e.g., [88, 90, 135]). They had paid attention to only radius of curvature in notch tip and ignored the notch shape in some vicinity of its tip.

Table 2.6 Values of stress rounding factor $R_{\mathrm{I}}(\beta)$ for rounded V-notch

2β	0°	1°	5°	10°	15°	30°	45°	60°
R_{I}	2.992	2.992	2.993	2.994	2.995	2.999	2.997	2.986
2β	75°	90°	105°	120°	135°	150°	165°	180°
R_{I}	2.957	2.901	2.806	2.659	2.439	2.123	1.677	1.000

2.5 Rounded V-Notch Under Mixed Loading

2.5.1 Antisymmetric Stress Distribution [204]

2.5.1.1 Problem Statement

Let the elastic plane contain sharp V-notch with the tip in coordinate system origin and vertex angle 2β $(0 \le 2\beta < \pi)$ (Fig. 2.8a). Assume that stress state of the notched plane is determined by complex potentials $\Phi_0^a(z)$ and $\Psi_0^a(z)$ (2.70), which ensure zero stresses at the notch contour L^0. Let us consider the smooth contour L composing of straight segments parallel to wedge faces L_0 and circular arc with radius ρ and center in the notch tip. Let us write the vector of normal (σ_n^0) and shear (τ_{ns}^0) stresses at this contour

$$\sigma_n^0 + i\tau_{ns}^0 = \Phi_0^a(t) + \overline{\Phi_0^a(t)} + \frac{\overline{\mathrm{d}t}}{\mathrm{d}t}\left[t\overline{\Phi_0'^a(t)} + \overline{\Psi_0^a(t)}\right] = -p(t), \quad t \in L^*. \tag{2.112}$$

Now consider the rounded V-notch with the same vertex angle and free of stresses contour L^* in the plane (Fig. 2.8b). Let an asymptotic stress distribution is given at infinity, which is determined by potentials

$$\Phi_0^a(z) = \frac{\mathrm{i}\tilde{K}_{\mathrm{II}}^{\mathrm{V}}}{(2\pi z^{\lambda_{\mathrm{II}}})}\frac{\sin 2\alpha}{\sin 2\lambda_{\mathrm{II}}\alpha - \lambda_{\mathrm{II}}\sin 2\alpha},$$
$$\Psi_0^a(z) = \frac{i\tilde{K}_{\mathrm{II}}^{\mathrm{V}}}{(2\pi z^{\lambda_{\mathrm{II}}})}\frac{\sin 2\lambda_{\mathrm{II}}\alpha}{\sin 2\lambda_{\mathrm{II}}\alpha - \lambda_{\mathrm{II}}\sin 2\alpha}. \tag{2.113}$$

We shall apply a superposition technique to solve this boundary value problem. Write above stress potentials in the form

$$\Phi_*(z) = \Phi_0^a(z) + \Phi(z), \qquad \Psi_*(z) = \Psi_0^a(z) + \Psi(z), \tag{2.114}$$

where functions $\Phi(z)$ and $\Psi(z)$ describe the disturbed stress state induced by a rounded V-notch L^*.

To find the disturbed stress state, we have to solve the boundary value problem for elastic plane containing the rounded V-notch with a contour L^*, at which the boundary condition

$$\sigma_n + \mathrm{i}\tau_{ns} = p(t), \qquad t \in L^*, \tag{2.115}$$

is satisfied, and stresses vanish at infinity. Stresses $p(t)$ here are determined from the formula (2.112).

2.5.1.2 Singular Integral Equation

Above-stated boundary value problem will be solved here using the method of singular integral equations similarly to previous case of symmetrical loading. Namely, we shall reduce it to boundary value problem for crack/notch along contour L, which, in limit case when the crack length approaches infinity, approaches the contour L^* (2.90). Integral representation of the solution is taken in the form (2.86). Satisfying the boundary conditions at crack edges, we get the singular integral equation of the problem

$$\frac{1}{\pi}\int\limits_L \left[K(t,t')g'(t)\,\mathrm{d}t + L(t,t')\overline{g'(t)}\,\mathrm{d}\bar{t}\right] = p(t'), \qquad t' \in L, \tag{2.116}$$

with kernels being given by the formulae (1.59).

A unique solution of integral equation (2.116) in class of functions, which have an integrable singularity at the ends of integration contours, exists if the additional condition is satisfied during tracing the crack contour

$$\int\limits_L g'(t)\,\mathrm{d}t = 0. \tag{2.117}$$

Solve the Eq. (2.116) numerically under condition (2.117) and get results for rounded V-notch (2.90) and hyperbolic notch (2.91). Write the Eqs. (2.116) and (2.117) in the canonical dimensionless form

$$\begin{cases} \dfrac{1}{\pi}\displaystyle\int\limits_{-1}^{1}[M(\xi,\eta)\phi(\xi) + N(\xi,\eta)\overline{\phi(\xi)}]\,\mathrm{d}\xi = p(\eta), \quad -1 \le \eta \le 1, \\ \dfrac{1}{\pi}\displaystyle\int\limits_{-1}^{1}\phi(\xi)\omega'(\xi)\,\mathrm{d}\xi = 0, \end{cases} \tag{2.118}$$

where

$$\begin{aligned} \phi(\xi) &= \frac{1}{\tau}\,g'(\rho\omega(\xi)), \\ M(\xi,\eta) &= \rho\omega'(\xi)\,K(\rho\omega(\xi),\rho), \\ N(\xi,\eta) &= \rho\overline{\omega'(\xi)}\,L(\rho\omega(\xi),\rho\omega(\eta)), \\ p(\eta) &= \frac{1}{\tau}p(\rho\omega(\eta)), \qquad \tau = \frac{\tilde{K}_{\mathrm{II}}^{\mathrm{V}}}{(2\pi\rho)^{\lambda_{\mathrm{II}}}}. \end{aligned} \tag{2.119}$$

Since we are considering the infinite contour L and in its ends (that is in points $\xi \pm 1$) unknown function $\phi(\xi)$ is constrained, we shall seek this function in the class

$$\phi(\xi) = \sqrt{1-\xi^2}\, u(\xi), \tag{2.120}$$

where $u(\xi)$ is a continuous function.

Solve the integral equation (2.118) numerically using quadrature method with quadrature formulae (1.108) and (1.109). As a result, we come to the system of $2n$ linear complex algebraic equations for $2n$ unknown functions $u(\xi_k)$ $(k = 1, \ldots, 2n)$

$$\begin{cases} \dfrac{1}{2n+1} \displaystyle\sum_{k=1}^{2n} w_k \left[M(\xi_k, \eta_m) u(\xi_k) + N(\xi_k, \eta_m) \overline{u(\xi_k)} \right] = p(\eta_m), \\ \qquad\qquad\qquad\qquad\qquad\qquad m = 1, \ldots, 2n-1, \\ \dfrac{1}{2n+1} \displaystyle\sum_{k=1}^{2n} w_k \omega'(\xi_k)\, u(\xi_k) = 0, \end{cases} \tag{2.121}$$

where

$$\begin{aligned} \xi_k &= \cos \frac{\pi k}{2n+1}, \qquad w_k = \sin^2 \frac{\pi k}{2n+1} = 1 - \xi_k^2, \\ \eta_m &= \cos \frac{\pi(2m+1)}{2(2n+1)}. \end{aligned} \tag{2.122}$$

Using the condition of antisymmetry

$$u(-\xi) = \overline{u(\xi)}, \tag{2.123}$$

we twice reduce order of the system (2.121)

$$\begin{cases} \dfrac{1}{2n+1} \displaystyle\sum_{k=1}^{n} w_k \left\{ [M(\xi_k, \eta_m) + N(-\xi_k, \eta_m)]\, u(\xi_k) + \right. \\ \qquad \left. + [N(\xi_k, \eta_m) + M(-\xi_k, \eta_m)]\, \overline{u(\xi_k)} \right\} = p(\eta_m), \\ \qquad\qquad\qquad\qquad\qquad\qquad m = 1, \ldots, n-1, \\ \dfrac{1}{2n+1} \mathrm{Im} \displaystyle\sum_{k=1}^{n} w_k \left\{ [M(\xi_k, 0) + N(-\xi_k, 0)]\, u(\xi_k) + \right. \\ \qquad \left. + [N(\xi_k, 0) + M(-\xi_k, 0)]\, \overline{u(\xi_k)} \right\} = \mathrm{Im}\ p(0), \\ \dfrac{1}{2n+1} \mathrm{Im} \displaystyle\sum_{k=1}^{n} w_k \omega'(\xi_k) u(\xi_k) = 0. \end{cases} \tag{2.124}$$

In deriving above relationship we had taken into account equalities

$$\omega'(\xi) = -\overline{\omega'(-\xi)}, \qquad \xi_{2n-k+1} = -\xi_k$$

as well as that normal stresses at axis Ox ($\eta_n = 0$) are zero (Re $p(0) = 0$) due to antisymmetry.

Similarly to symmetrical case, here we get the formula for stress σ_s^*

$$\sigma_s^* = 4\mathrm{Re}\,\left[\Phi_0^a(t) + \Phi^-(t)\right], \tag{2.125}$$

which, after substitution, takes the form

$$\sigma_s^*(\eta) = \frac{\tilde{K}_{\mathrm{II}}^{\mathrm{V}}}{(2\pi\rho)^{\lambda_{\mathrm{II}}}}\mathrm{Re}\,\left[\frac{4\mathrm{i}}{(\omega(\eta))^{\lambda_{\mathrm{II}}}}\frac{\sin 2\alpha}{\sin 2\lambda_{\mathrm{II}}\alpha - \lambda_{\mathrm{II}}\sin 2\alpha} - \frac{2\mathrm{i}u(\eta)\sqrt{1-\eta^2}}{\omega'(\eta)} + \right.$$
$$\left. + \frac{2}{\pi}\int\limits_{-1}^{1}\frac{\sqrt{1-\xi^2}u(\xi)}{\omega(\xi)-\omega(\eta)}\,\mathrm{d}\xi\right] = \frac{\tilde{K}_{\mathrm{II}}^{\mathrm{V}}}{(2\pi\rho)^{\lambda_{\mathrm{II}}}}R_{\mathrm{II}}(\eta). \tag{2.126}$$

Using the condition of antisymmetry (2.123), we can find dimensionless stress $R_{\mathrm{II}}(\eta_m)$ in nodes η_m, $(m = 1, \ldots, n-1)$ from the formula

$$R_{\mathrm{II}}(\eta_m) = \mathrm{Re}\,\left\{\frac{4\,\mathrm{i}}{(\omega(\eta_m))^{\lambda_{\mathrm{II}}}}\frac{\sin 2\alpha}{\sin 2\lambda_{\mathrm{II}}\alpha - \lambda_{\mathrm{II}}\sin 2\alpha} - 2\mathrm{i}\sqrt{1-\eta_m^2}\,u(\eta_m) + \right.$$
$$\left. + \frac{4}{2n+1}\sum_{k=1}^{n} w_k\left[\frac{\omega'(\xi_k)u(\xi_k)}{\omega(\xi_k)-\omega(\eta_m)} - \frac{\overline{\omega'(\xi_k)u(\xi_k)}}{\overline{\omega(\xi_k)}-\omega(\eta_m)}\right]\right\}. \tag{2.127}$$

Values of the function $u(\eta)$ in nodes η_m can be calculated using Lagrangian interpolation formula, which becomes after considering the condition (2.123) into

$$u(\eta_m) = \frac{1}{(2n+1)\sqrt{1-\eta_m^2}}\sum_{k=1}^{n}(-1)^{m+k}(1-\xi_k^2)\left[\frac{\overline{u(\xi_k)}}{\eta_m+\xi_k} - \frac{u(\xi_k)}{\eta_m-\xi_k}\right] \tag{2.128}$$

2.5.1.3 Numerical Results

Stresses at notch contours σ_s were found in nodes η_m $(m = 1, \ldots, n)$. Changing to polar coordinates r, θ with the pole in point $z = 0$, we obtain $\sigma_s^*(\theta_m) = \sigma_s^*(\eta_m)$, $\theta_m = \arg(t_m)$, $t_m = \rho\omega(\eta_m)$. Dependence of dimensionless stress $R_{\mathrm{II}}(\theta) = -R_{\mathrm{II}}(-\theta)$ (2.127) at upper branch of boundary contour on angular coordinate θ $(0 \le \theta \le \alpha^*)$ for both notches at various values of their vertex angles 2β is illustrated in Fig. 2.14.

It can be concluded while comparing presented data for rounded V-notch and hyperbolic notch at the same radii of curvature ρ and vertex angles 2β in the notch tip that there is a great difference between them at antisymmetrical distribution.

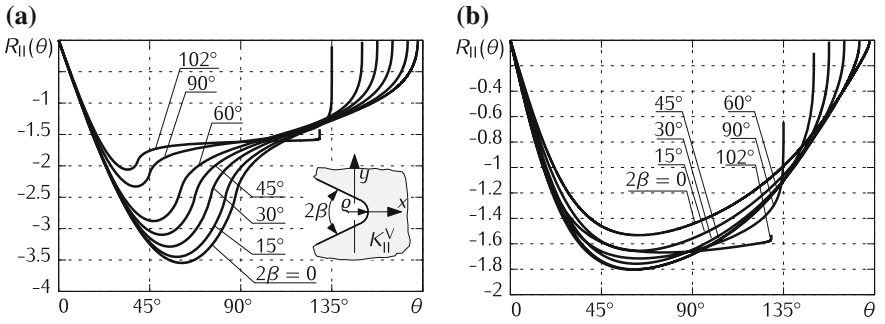

Fig. 2.14 Dimensionless stress distribution $R_{II}(\theta)$ along contours of rounded V-notch (**a**) or hyperbolic notch (**b**)

Extremal stress values differ more than twice in both cases. Note that presented solution for hyperbolic notch well agree with the known data [15].

If parameter $\lambda_{II} > 0$, then stresses σ_s have a local extremum in vicinity of notch tip and approach zero at infinity ($\xi \to 1$). In the limit case when angle $\beta \to \beta^*$ ($\lambda_{II} \to 0$), stresses σ_s^* at infinity approach a definite value coinciding with the stress $\sigma_{rr}(\alpha^*)$ (2.34)

$$\sigma_{rr}(\alpha^*) = \frac{3\alpha^* \sin 2\alpha^*}{2\alpha^* - \sin 2\alpha^*} \tilde{K}_{II}^{V} = -\frac{3\alpha^*}{\sqrt{1 + 4(\alpha^*)^2} + 1} \tilde{K}_{II}^{V} \approx -1.203\, \tilde{K}_{II}^{V}. \quad (2.129)$$

Extremal values of dimensionless stresses $R_{II} = R_{II}(\theta_{max})$ (Fig. 2.15b) are reached in points θ_{max} (Fig. 2.15a) at some distance from the notch tip.

For U-shaped notch ($\beta = 0$), extremal values of dimensionless stresses $R_{II} = -3.592$ are attained when $\theta = 1,082$. Obtained values for hyperbolic notch are in very good accordance with known results [15] at individual notch vertex angles

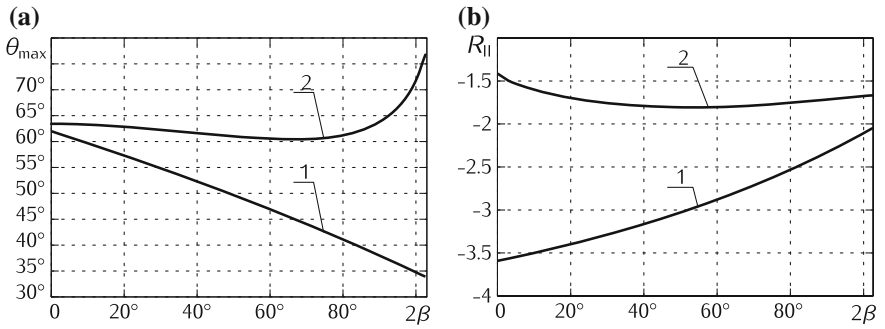

Fig. 2.15 Dependencies of angular coordinate θ_{max} (**a**) and respective dimensionless stress $R_{II} = R_{II}(\theta_{max})$ (**b**) on notch vertex angle 2β (1 – rounded V-notch; 2 – hyperbolic notch)

2β. At $\beta = 0$, hyperbolic notch transforms into the parabolic one, which has a well-known closed analytical solution (2.53).

Similarly to derivation of relationship (2.23), we can derive here the interrelation between circular stress gradient in the notch tip and stress intensity factor $\tilde{K}_{\mathrm{II}}^{\mathrm{V}}$

$$\left.\frac{\mathrm{d}\sigma_s^*(\theta)}{\mathrm{d}\theta}\right|_{\theta=0} = \frac{\tilde{K}_{\mathrm{II}}^{\mathrm{V}}}{(2\pi\rho)^{\lambda_{\mathrm{II}}}} \left.\frac{\mathrm{d}R_{\mathrm{II}}(\theta)}{\mathrm{d}\theta}\right|_{\theta=0} = \frac{\tilde{K}_{\mathrm{II}}^{\mathrm{V}}}{(2\pi\rho)^{\lambda_{\mathrm{II}}}} R'_{\mathrm{II}}. \tag{2.130}$$

Note that at circular segment of rounded V-notch contour (2.90) angular coordinate $\theta = \xi\alpha$.

Dependencies of dimensionless stress gradient R'_{II} in the tip of rounded V-notch or hyperbolic notch on notch vertex angle 2β are shown in Fig. 2.16. For U-shaped notch ($\beta = 0$) we have: $R'_{\mathrm{II}} = -5.186$.

The angular coordinate of a contour point, in which extremal stresses are reached, normalized by circular stress gradient in notch tip ($\theta_{\max}/R'_{\mathrm{II}}$) depends on vertex angle 2β, as shown in Fig. 2.17. For U-shaped notch ($\beta = 0$) we have $\theta_{\max}/R'_{\mathrm{II}} = -0.209$.

In conclusion, we can find stress intensity factor in symmetrical region with sharp V-notch under antisymmetrical loading using a limit transition from corresponding rounded notch when rounding radius approaches zero, for which relationships for

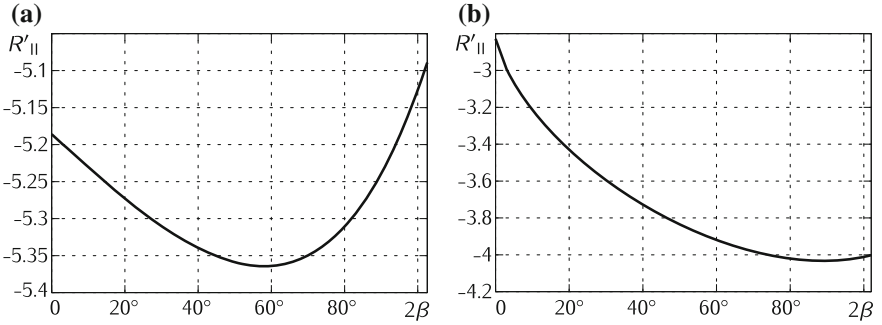

Fig. 2.16 Dimensionless stress gradient R'_{II} in the tip of rounded V-notch (**a**) or hyperbolic notch (**b**) with respect to notch vertex angle 2β

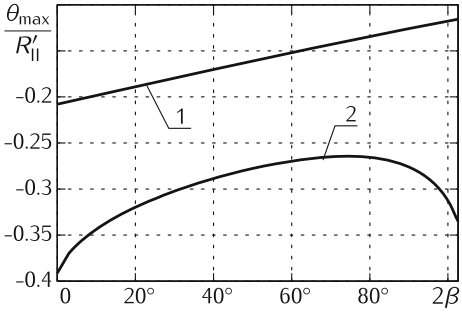

Fig. 2.17 Dependence of ratio $\theta_{\max}/R'_{\mathrm{II}}$ on notch vertex angle 2β (1 – rounded V-notch, 2 – hyperbolic notch)

extremal dimensionless stresses R_{II} (Fig. 2.15b) or their gradient R'_{II} in rounded notch tip (Fig. 2.16) were derived.

2.5.2 Complex-Stressed State [205]

When elastic region is symmetrical with respect to V-notch bisecting line, the problem can be divided into two problems for symmetrical and antisymmetrical loading at any scheme of applied loading. On the contrary, when elastic region is asymmetrical, stresses on the boundary contour can attain extremal values at various distances from notch tip depending on interrelation between stress intensity factors $\tilde{K}_{\mathrm{I}}^{\mathrm{V}}$ and $\tilde{K}_{\mathrm{II}}^{\mathrm{V}}$, which precludes usage of obtained extremal stresses dependence on rounding radius ρ in the above-mentioned limit transitions. In this case we have a complex-stressed state in the notch tip that requires conceptually another approach, if both stress intensity factors $\tilde{K}_{\mathrm{I}}^{\mathrm{V}}$ and $\tilde{K}_{\mathrm{II}}^{\mathrm{V}}$ are nonzero.

A unified approach is proposed in this section to solve plane problems of elasticity theory for bodies with sharp or rounded V-notches under complex-stressed state. We have built interrelations between stress intensity factors $\tilde{K}_{\mathrm{I}}^{\mathrm{V}}$ and $\tilde{K}_{\mathrm{II}}^{\mathrm{V}}$ in the sharp V-notch tip, stresses, and their gradient at the boundary contour in the tip of corresponding rounded notch. These interrelations for finite bodies are of asymptotic nature when radius of curvature in the notch tip approaches zero, which opens a possibility to find SIF in the sharp notch tip based on data about stress and its gradient in the tip of rounded notch. As soon as stress intensity factor in the sharp notch tip become known, the derived relations allow estimating stress concentration near rounded V-notch with small relative rounding radius in the tip, if obtaining the numerical solution encounters great difficulties of computational nature.

Let the elastic plane be weakened with a semi-infinite V-shaped rounded notch (Fig. 2.8b). We shall assume that the boundary of the elastic region is free of applied loads and an asymptotic stress field is given at infinity, which is determined by complex potentials

$$\begin{aligned}\Phi_0(z) &= -\frac{\tilde{K}_{\mathrm{I}}^{\mathrm{V}}}{(2\pi z)^{\lambda_{\mathrm{I}}}}\frac{\sin 2\alpha}{(\lambda_{\mathrm{I}}-2)\sin 2\alpha+\sin 2\lambda_{\mathrm{I}}\alpha}\\ &\quad+\frac{\mathrm{i}\tilde{K}_{\mathrm{II}}^{\mathrm{V}}}{(2\pi z)^{\lambda_{\mathrm{II}}}}\frac{\sin 2\alpha}{\sin 2\lambda_{\mathrm{II}}\alpha-\lambda_{\mathrm{II}}\sin 2\alpha},\\ \Psi_0(z) &= \frac{\tilde{K}_{\mathrm{I}}^{\mathrm{V}}}{(2\pi z)^{\lambda_{\mathrm{I}}}}\frac{\sin(2\lambda_{\mathrm{I}}\alpha)}{(\lambda_{\mathrm{I}}-2)\sin 2\alpha+\sin 2\lambda_{\mathrm{I}}\alpha}\\ &\quad+\frac{\mathrm{i}\tilde{K}_{\mathrm{II}}^{\mathrm{V}}}{(2\pi z)^{\lambda_{\mathrm{II}}}}\frac{\sin 2\lambda_{\mathrm{II}}\alpha}{\sin 2\lambda_{\mathrm{II}}\alpha-\lambda_{\mathrm{II}}\sin 2\alpha},\end{aligned}\tag{2.131}$$

when both stress intensity factors $\tilde{K}_{\mathrm{I}}^{\mathrm{V}}$ and $\tilde{K}_{\mathrm{II}}^{\mathrm{V}}$ are nonzero. So stated problem can be interpreted also in somewhat another manner. Let an elastic wedge in a stress–strain

state characterized by complex potentials (2.131) have a cut along the contour L (Fig. 2.8b). We have to find the disturbed stress state induced by a rounded V-notch with boundary contour L in elastic plane (or wedge). Since the elastic region is symmetrical with respect to axis Ox, the problem can be divided into two problems, symmetrical and antisymmetrical. As outlined above, solutions to these problems were found using the singular integral equation method for notch contour that can be described by the following parametric equation:

$$t = \rho\omega(\xi), \qquad -1 < \xi < 1, \tag{2.132}$$

where ρ is radius of notch tip curvature, $t = x + iy \in L$.

Numerical results were obtained for rounded V-notches (2.90) and hyperbolic (2.91) notches. Tangential normal stresses at notch contour L can be represented in the form [205, 210]

$$\sigma_s(\theta) = \frac{\tilde{K}_{\mathrm{I}}^{\mathrm{V}}}{(2\pi\rho)^{\lambda_{\mathrm{I}}}} R_{\mathrm{I}}(\theta, \beta) + \frac{\tilde{K}_{\mathrm{II}}^{\mathrm{V}}}{(2\pi\rho)^{\lambda_{\mathrm{II}}}} R_{\mathrm{II}}(\theta, \beta) \tag{2.133}$$

where $R_{\mathrm{I}}(\theta, \beta) = R_{\mathrm{I}}(-\theta, \beta) = R_{\mathrm{I}}(\theta)$ (Fig. 2.18) and $R_{\mathrm{II}}(\theta, \beta) = -R_{\mathrm{II}}(-\theta, \beta) = R_{\mathrm{II}}(\theta)$ (Fig. 2.14) are dimensionless stresses under symmetrical or antisymmetrical distributions, respectively. Note that although stress distribution along notch contour under symmetrical loading had been shown earlier in Fig. 2.11, we shall use the dependence on polar angle θ for further analysis, which is more convenient in calculations.

The conclusion follows from representation (2.133) that stress intensity factors $\tilde{K}_{\mathrm{I}}^{\mathrm{V}}$ and $\tilde{K}_{\mathrm{II}}^{\mathrm{V}}$ determine stress distribution in elastic body weakened by respective smooth curvilinear notch at small relative rounding radii of the notch tip. It was already mentioned above that these factors determine stress–strain state near sharp tip of V-shaped notch in elastic body too. These facts explain the great role, which stress intensity factors are playing in fracture mechanics.

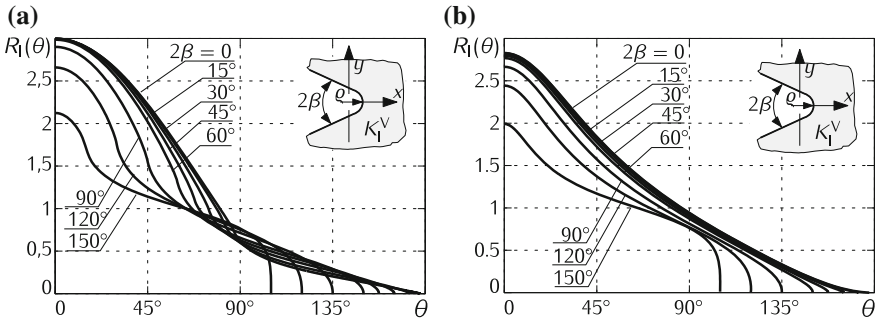

Fig. 2.18 Dimensionless stress distribution $R_{\mathrm{I}}(\theta)$ along contour L of rounded V-notch (**a**) or hyperbolic notch (**b**)

It can be concluded while comparing presented data for rounded V-notch and hyperbolic notch at the same radii of curvature ρ and vertex angles 2β in the notch tip that there is a great difference between them at antisymmetrical distribution than at symmetrical one. Extremal stress values in antisymmetrical case differ more than by two times. On contrary, relative difference in maximal stresses in notch tip under symmetrical loading is below 15 %.

Consequently, notch contour shape in vicinity of its tip essentially effects on stress distribution. Therefore, studying into stress concentration near V-shaped rounded notches as most important for practice (more precisely, having shape of wedge with straight edges rounded in vertex with circular arc) is very urgent. Advantages of proposed approach are clearly seen when obtained results are used as asymptotic solutions at small relative V-notch rounding radii in finite bodies.

Let us confine ourselves with considering only rounded V-notches. Fitting formulae for dimensionless stresses $R_{\mathrm{I}}(\theta)$ and $R_{\mathrm{II}}(\theta)$ in the interval $0 \le \theta \le \theta^*$, where stresses $\sigma_s(\theta)$ attain maximal values at complex-stressed state ($\tilde{K}_{\mathrm{I}}^{\mathrm{V}} \neq 0$, $\tilde{K}_{\mathrm{II}}^{\mathrm{V}} \neq 0$), have the following form

$$\begin{aligned} R_{\mathrm{I}}(\theta) &= a_{\mathrm{I}} + b_{\mathrm{I}}\theta^2 + c_{\mathrm{I}}\theta^4, \\ R_{\mathrm{II}}(\theta) &= a_{\mathrm{II}}\theta + b_{\mathrm{II}}\theta^3 + c_{\mathrm{II}}\theta^5, \quad 0 \le \theta \le \theta^* \end{aligned} \tag{2.134}$$

Here θ^* is the angle, at which stresses $\sigma_s(\theta)$ attain extremal values at $\tilde{K}_{\mathrm{I}}^{\mathrm{V}} = 0$. Coefficients a_{I}, a_{II}, b_{I}, b_{II}, and c_{I}, c_{II} can be presented in analytical form using values of dimensionless stresses $R_{\mathrm{I}}(\theta)$ and $R_{\mathrm{II}}(\theta)$ and their derivatives in notch tip ($\theta = 0$) and in the point $\theta = \theta^*$

$$\begin{aligned} a_{\mathrm{I}} &= R_{\mathrm{I}}, \quad & b_{\mathrm{I}} &= \frac{-4\,R_{\mathrm{I}} + 4\,R_{\mathrm{I}}^* - R'^*_{\mathrm{I}}\theta^*}{2\theta^{*2}}, \quad & c_{\mathrm{I}} &= \frac{2\,R_{\mathrm{I}} - 2\,R_{\mathrm{I}}^* + R'^*_{\mathrm{I}}\theta^*}{2\theta^{*4}}, \\ a_{\mathrm{II}} &= R'_{\mathrm{II}}, \quad & b_{\mathrm{II}} &= \frac{5\,R_{\mathrm{II}}^* - 4\,R'_{\mathrm{II}}\theta^*}{2\theta^{*3}}, & c_{\mathrm{II}} &= \frac{-3\,R_{\mathrm{II}}^* + 2R'_{\mathrm{II}}\theta^*}{2\theta^{*5}}, \end{aligned} \tag{2.135}$$

$$\begin{aligned} &R_{\mathrm{I}} = R_{\mathrm{I}}(0), \qquad R_{\mathrm{I}}^* = R_{\mathrm{I}}(\theta^*), \qquad R'^*_{\mathrm{I}} = \left.\frac{\mathrm{d}R_{\mathrm{I}}(\theta)}{\mathrm{d}\theta}\right|_{\theta=\theta^*}, \\ &R'_{\mathrm{II}} = \left.\frac{\mathrm{d}R_{\mathrm{II}}(\theta)}{\mathrm{d}\theta}\right|_{\theta=0}, \quad R_{\mathrm{II}}^* = R_{\mathrm{II}} = R_{\mathrm{II}}(\theta^*). \end{aligned} \tag{2.136}$$

Fitting formulae for above-used parameters have the form

$$\begin{aligned} \theta^* &= 2.081 - \exp(0.445\beta), \\ R_{\mathrm{I}} &= 2.993 + 0.1810\beta^2 - 0.3694\beta^3 - 0.08291\beta^5, \\ R_I^* &= 1.668 + 0.7049\beta - 0.3286\beta^2 - 0.9378\beta^5, \\ R'^*_{\mathrm{I}} &= -2.004 - 0.297\beta - 0.7830\beta^2 - 0.3101\beta^5, \quad 0 \le \beta \le \pi, \end{aligned}$$

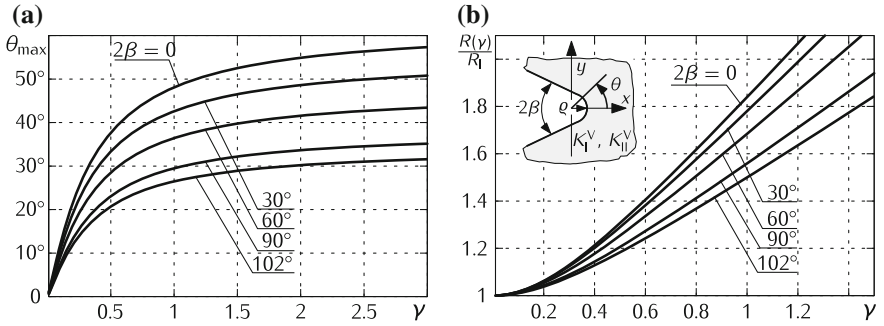

Fig. 2.19 Dependencies of angle θ_{max} (**a**) and dimensionless maximal stress $R(\gamma)/R_I$ (**b**) on parameter γ for various vertex angles 2β

$$R_{II}^* = R_{II} = 4.467 - 0.875\exp(1.137\beta),$$
$$R'_{II} = 5.234\exp(0.137\beta) - 0.051\exp(3.114\beta), \quad 0 \le \beta \le \beta^*, \qquad (2.137)$$

with relative error below 0.5 %.

Locations of points θ_{max} (Fig. 2.19a), where maximal stresses $R(\gamma) = \sigma_s(\theta_{max})$ (Fig. 2.19b) are reached, depend on parameter $\gamma = \rho^{\lambda_I - \lambda_{II}} K_{II}^V / K_I^V$. Based on relationship (2.133), we get the approximate formula for the angle θ_{max}

$$\theta_{max}(\gamma) = \frac{\theta^*}{2}\left\{1 + \tanh\left[0.5822\ln(\gamma) + 0.6222\right]\right\}, \qquad 0 \le \gamma < \infty. \qquad (2.138)$$

Corresponding maximal values of tangential stresses at notch contour can be found using the formula (2.133), if putting $\theta = \theta_{max}$ in it.

Obtained solutions to singular boundary value problem for semi-infinite rounded V-shaped notch can be used as asymptotic relations for finite bodies with V-shaped cracks/holes, when relative rounding radii are small. Having found stress intensity factors $\tilde{K}_I^V$ and $\tilde{K}_{II}^V$, one can easily examine stress concentration in vicinity of notch tip with small radius of curvature using relationships from (2.133) to (2.138) just in that very case when obtaining the solution encounters great computational difficulties. On the other hand, these relationships can be alternatively used to find SIF in the sharp notch tip based on solutions for respective rounded notches and limit transitions

$$\tilde{K}_I^V = \frac{1}{R_I}\lim_{\rho\to 0}\left[(2\pi\rho)^{\lambda_I}\sigma_s^*(0)\right],$$
$$\tilde{K}_{II}^V = \frac{1}{R'_{II}}\lim_{\rho\to 0}\left[(2\pi\rho)^{\lambda_{II}}\frac{d\sigma_s^*(\theta)}{d\theta}\bigg|_{\theta=0}\right]. \qquad (2.139)$$

In the next chapters, applications of this approach will be illustrated with examples of acute-angled holes and sharp V-shaped notches in elastic regions.

References

1. Akin, J.E.: The generation of elements with singularities. Int. J. Numer. Methods Eng. **10**, 1249–1259 (1976)
2. Aleksandrov, A.Y., Zinov'ev, B.M., Kurshin, L.M.: One numerical method of solving problems of elasticity with allowance for singularities of the stresses state near corner points and lines. Mech. Solids **15**(3), 39–49 (1980)
3. Aleksanyan, R.K.: On a class of solutions of the equations of the plane theory of elasticity of an anisotropic body. Rep. Acad. Sci. Armen. SSR **61**(4), 219–224 (1975)
4. Aleksanyan, R.K., Gevorkyan, S.H.: On the first fundamental problem of plane theory of elasticity for anisotropic wedge. Proc. Natl. Acad. Sci. Armen. Mech. **53**(2), 10–15 (2000)
5. Atkinson, C., Bourne, J.P.: Stress singularities in angular sectors of viscoelastic media. Int. J. Eng. Sci. **28**(7), 615–630 (1990)
6. Atzori, B., Lazzarin, P.: Notch sensitivity and defect sensitivity under fatigue loading: two sides of the same medal. Int. J. Fract. **107**, L3–L8 (2000)
7. Ayatollahi, M.R., Nejati, M.: Determination of NSIFs and coefficients of higher order terms for sharp notches using finite element method. Int. J. Mech. Sci. **53**(3), 164–177 (2011)
8. Banks-Sills, L., Sherer, A.: A conservative integral for determining stress intensity factors of a bimaterial notch. Int. J. Fract. **115**(1), 1–25 (2002)
9. Banks-Sills, L., Yang, Y.Y., Munz, D.: An influence function for stress intensity factors of bimaterial notched bodies. Int. J. Fract. **85**(4), 333–350 (1997)
10. Bansal, A., Kumosa, M.: Analysis of double edge-cracked iosipescu specimens under biaxial loads. Eng. Fract. Mech. **59**(1), 89–100 (1998)
11. Barber, J.R.: Elasticity, 2nd edn. Kluwer Academic Publishers, New York (2002)
12. Barone, M.R., Robinson, A.R.: Determination of elastic stresses at notches and cornes by integral equations. Int. J. Solids Struct. **8**, 1319–1338 (1972)
13. Belubekyan, V.M., Belubekyan, M.V., Terzyan, S.A.: Stress state in the vicinity of the elastic wedge vertex. Proc. Natl. Acad. Sci. Armen. Mech. **54**(2), 8–21 (2001)
14. Benthem, J.: On the stress distribution in anisotropic infinite wedges. Q. Appl. Math. **21**(3), 189–198 (1963)
15. Benthem, J.P.: Stresses in the region of rounded corners. Int. J. Solids Struct. **23**(2), 239–252 (1987)
16. Berto, F., Lazzarin, P., Matvienko, Y.G.: J-integral evaluation for U- and V-blunt notches under mode I loading and materials obeying a power hardening law. Int. J. Fract. **146**(1), 33–51 (2007)
17. Blanco, C., Martinez-Esnaola, J.M., Atkinson, C.: Analysis of sharp angular notches in anisotropic materials. Int. J. Fract. **93**(1–4), 373–386 (1998)
18. Blinowski, A., Rogaczewski, J.: On the order of singularity at V-shaped notches in anisotropic bodies. Arch. Mech. **52**(6), 1001–1010 (2000)
19. Blinowski, A., Wieromiej-Ostrowska, A.: On the singularities at the tips of orthotropic wedges in plane elasticity - I. Technol. Sci. **8**, 107–124 (2005)
20. Bogy, D.B.: Edge-bonded dissimilar orthogonal elastic wedges under normal and shear loading. J. Appl. Mech. **35**, 460–466 (1968)
21. Bogy, D.B.: Two edge-bonded elastic wedges of different materials and wedge angles under surface tractions. J. Appl. Mech. **38**, 377–386 (1968)
22. Bogy, D.B.: The plane solution for anisotropic elastic wedges under normal and shear loading. J. Appl. Mech. **39**, 1103–1109 (1972)
23. Bogy, D.B., Wang, K.C.: Stress singularities at interface corners in bonded dissimilar isotropic elastic materials. Int. J. Solids Struct. **7**(8), 993–1005 (1971)
24. Bourne, J.P., Atkinson, C.: Stress singularities in viscoelastic media 2. Plane-strain stress singularities at corners. IMA J. Appl. Math. **44**(2), 163–180 (1990)
25. Brahtz, A.H.A.: Stresses at two-dimensional corners for various force distributions. Ph.D. thesis, California Institute of Technology, Pasadena California (1932)

26. Brahtz, J.H.A.: Stress distribution in a reentrant corner. Trans. ASME **55**, 31–37 (1933)
27. Brahtz, J.H.A.: Stress distribution in wedges with arbitrary boundary forces. J. Appl. Phys. **4**(2), 56–65 (1933)
28. Broberg, K.B.: Cracks and Fracture. Academic Press, San Diego (1999)
29. Carpenter, W.C.: Calculation of fracture parameters for a general corner. Int. J. Fract. **24**(1), 45–58 (1984)
30. Carpenter, W.C.: A collocation procedure for determining fracture mechanics parameters at a corner. Int. J. Fract. **24**(4), 255–266 (1984)
31. Carpenter, W.C.: Mode I and mode II stress intensities for plates with cracks of finite opening. Int. J. Fract. **26**(3), 201–214 (1984)
32. Carpenter, W.C.: The eigenvector solution for a general corner or finite opening crack with further studies on the collocation procedure. Int. J. Fract. **27**, 63–73 (1985)
33. Carpenter, W.C.: Comments on the eigenvalue formulation of problems with cracks, V-notched cracks, and corners. Int. J. Fract. **68**(1), 75–87 (1994)
34. Carpenter, W.C., Byers, C.: Path independent integral for computing stress intensities for V-notched cracks in a bi-material. Int. J. Fract. **35**(4), 245–268 (1987)
35. Carpinteri, A., Paggi, M., Pugno, N.: Numerical evaluation of generalized stress intensity factors in multi-layered composites. Int. J. Solids Struct. **43**(3–4), 627–641 (2006)
36. Cartwright, D.J., Rooke, D.P.: Evaluation of stress intensity factors. J. Strain Anal. **10**(4), 217–224 (1975)
37. Chang, J.H., Wu, W.H.: Calculation of mixed-mode stress filed at a sharp notch tip using $M_{1\varepsilon}$-integral. Comput. Mech. **31**, 419–427 (2003)
38. Chao, Y.J., Yang, S.: Singularities at the apex of a sharp V-notch in a linear strain hardening material. Int. J. Fract. **57**(1), 47–60 (1992)
39. Chen, D., Ushijima, K.: Plastic stress singularity near the tip of a V-notch. Int. J. Fract. **106**(2), 117–134 (2000)
40. Chen, D.H., Nisitani, H.: Mode I and II singular stress fields near a corner of jointed dissimilar materials. JSME Int. J. **35**, 392–398 (1992)
41. Chen, D.H., Nisitani, H.: Singular stress field near the corner of jointed dissimilar materials. J. Appl. Mech. **60**(3), 607–613 (1993)
42. Chen, D.H., Nisitani, H.: Body force method. Int. J. Fract. **86**(1), 161–189 (1997)
43. Chen, Y.H., Lu, T.J.: On the path dependence of the J-integral in notch problems. Int. J. Solids Struct. **41**, 607–618 (2004)
44. Cheng, C., Niu, Z., Zhou, H., Recho, N.: Evaluation of multiple stress singularity orders of a V-notch by the boundary element method. Eng. Anal. Bound. Elem. **33**(10), 1145–1151 (2009)
45. Cherepanov, G.P.: Mekhanika khrupkogo razrusheniya (Mechanics of brittle fracture). Nauka, Moscow (1974)
46. Cherepanov, G.P.: Mechanics of Brittle Fracture. McGraw Hill, New York (1979)
47. Chiang, C.R.: Stress field around a rounded crack tip. J. Appl. Mech. **58**(3), 834–836 (1991)
48. Chiang, C.R.: The stress field for a blunt crack in an anisotropic material. Int. J. Fract. **68**(2), R41–R46 (1994)
49. Cho, S.B., Kim, J.K.: A study on stress singularities for V-notched cracks in anisotropic and/or pseudo-isotropic dissimilar materials. Int. J. Korean Soc. Precis. Eng. **3**(2), 22–32 (2002)
50. Chuang, W.Y., Sung, J.C., Chung, W.G.: Stress singularities of two special geometries of wedges with free-mixed boundary conditions. Comput. Struct. **81**(3), 167–176 (2003)
51. Chue, C.H., Liu, C.I.: A general solution on stress singularities in an anisotropic wedge. Int. J. Solids Struct. **38**(38–39), 6889–6906 (2001)
52. Chue, C.H., Liu, C.I.: Stress singularities in a bimaterial anisotropic wedge with arbitrary fiber orientation. Compos. Struct. **58**(1), 49–56 (2002)
53. Chue, C.H., Weng, S.M.: Stress singularities in anisotropic three-material wedges and junctions with applications. Compos. Struct. **58**(4), 443–456 (2002)
54. Chue, C.H., Tseng, C.H., Liu, C.I.: On stress singularities in an anisotropic wedge for various boundary conditions. Compos. Struct. **54**, 87–102 (2001)

55. Cormack, D.E., Rosen, D.: Gauge conditions and the analysis of singular fields with boundary integral equations. Eng. Anal. Bound. Elem. **18**(1), 1–8 (1996)
56. Creager, M., Paris, P.C.: Elastic field equations for blunt cracks with reference to stress corrosion cracking. Int. J. Fract. Mech. **3**, 247–252 (1967)
57. De Chen, C., Chue, C.H.: Singular stresses near apex of wedge by finite element analysis. J. Chin. Inst. Eng. **26**(4), 423–434 (2003)
58. Della-Ventura, D., Smith, R.N.L.: Some applications of singular fields in the solution of crack problems. Int. J. Numer. Methods Eng. **42**, 927–942 (1998)
59. Dempsey, J., Sinclair, G.: On the stress singularities in the plane elasticity of the composite wedge. J. Elast. **9**(4), 373–391 (1979)
60. Dempsey, J., Sinclair, G.: On the singular behavior at the vertex of a bi-material wedge. J. Elast. **11**(3), 317–327 (1981)
61. Denisyuk, I.T.: Stress singularities of anisotropic plates with angular cuts. Int. Appl. Mech. **32**(1), 41–45 (1996)
62. Ding, S., Meekisho, L., Kumosa, M.: Analysis of stress singular fields at a bimaterial wedge corner. Eng. Fract. Mech. **49**(4), 569–585 (1994)
63. Dini, D., Hills, D.: The effect of a crack-tip radius on the validity of the singular solution. Proc. Inst. Mech. Eng. Part C: Mech. Eng. Sci. **218**(7), 693–701 (2004)
64. Dini, D., Hills, D.: When does a notch behave like a crack? Proc. Inst. Mech. Eng. Part C: Mech. Eng. Sci. **220**(1), 27–43 (2006)
65. Dini, D., Hills, D.A.: Asymptotic characterization of nearly-sharp notch root stress fields. Int. J. Fract. **130**, 651–666 (2004)
66. Dundurs, J.: Effect of elastic constants on stress in a composite under plane deformation. J. Compos. Mater. **1**(3), 310–322 (1967)
67. Elliott, D., Johnston, P.R.: Error analysis for a sinh transformation used in evaluating nearly singular boundary element integrals. J. Comput. Appl. Math. **203**(1), 103–124 (2007)
68. Elliott, D., Johnston, P.R.: Gauss-Legendre quadrature for the evaluation of integrals involving the Hankel function. J. Comput. Appl. Math. **211**(1), 23–35 (2008)
69. Elschner, J., Stephan, E.P.: A discrete collocation method for Symm's integral equation on curves with corners. J. Comput. Appl. Math. **75**(1), 131–146 (1996)
70. Fan, Z., Long, Y.: Sub-region mixed finite element analysis of V-notched plates. Int. J. Fract. **56**, 333–344 (1992)
71. Fett, T.: Weight function for cracks ahead of sharp notches. Int. J. Fract. **74**(1), 11–16 (1995)
72. Fett, T.: Weight functions for cracks at sharp notches and notch intensity factors. Int. J. Fract. **77**, R27–R33 (1996)
73. Fett, T., Munz, D.: Stress intensity factors and weight functions. Advances in Fracture Mechanics. Computational Mechanics Publications Inc., Southampton (1997)
74. Filippi, S., Ciavarella, M., Lazzarin, P.: An approximate, analytical approach to the 'HRR'-solution for sharp V-notches. Int. J. Fract. **117**(3), 269–286 (2002)
75. Filippi, S., Lazzarin, P., Tovo, R.: Developments of some explicit formulas useful to describe elastic stress fields ahead of notches in plates. Int. J. Solids Struct. **39**(17), 4543–4565 (2002)
76. Fukui, T.: On corner solutions by indirect BIEM. Boundary elements V. In: Proceedings of the 5th International Conference, pp. 929–938. Springer, Berlin (1983)
77. Gecit, M.R.: An integral equation approach for simultaneous solution of rectangular hole and rectangular block problems. Int. J. Eng. Sci. **21**(9), 1041–1051 (1983)
78. Gevorkyan, S.K.: Investigation of singularities in the solutions of some problems of the theory of elasticity for anisotropic solids. Proc. Nat. Acad. Sci. Armen. Mech. **21**(4), 30–39 (1968)
79. Givoli, D., Rivkin, L.: The DtN finite element method for elastic domains with cracks and entrant corners. Comput. Struct. **49**, 633–642 (1993)
80. Givoli, D., Rivkin, L., Keller, J.B.: A finite element method for domains with corners. Int. J. Numer. Methods Eng. **35**(6), 1329–1345 (1992)
81. Glinka, G.: Energy density approach to calculation of inelastic strain-stress near notches and cracks. Eng. Fract. Mech. **22**(3), 485–508 (1985)

82. Glinka, G., Ott, W., Nowack, H.: Elastoplastic plane strain analysis of stresses and strains at the notch root. J. Eng. Mater. Technol. **110**, 195–204 (1988)
83. Gómez, F.J., Elices, M.: A fracture criterion for blunted V-notched samples. Int. J. Fract. **127**(3), 239–264 (2004)
84. Gospodinov, G., Drakaliev, P., Kerelezova, I.: A singular boundary element for a general corner case. In: Proceedings of the Anniversary Scientific Conference 50 Faculty of Hydrotechnics of the University of Architecture, Civil Engineering and Geodesy, Sofia, pp. 113–120 (1999)
85. Gross, B., Mendelson, A.: Plane elastostatic analysis of V-notched plates. Int. J. Fract. Mech. **8**(3), 267–276 (1972)
86. Groth, H.: Stress singularities and fracture at interface corners in bonded joints. Int. J. Adhes. Adhes. **8**(2), 107–113 (1988)
87. Gumerov, K.M., Kolesov, A.V., Gnidin, V.A.: Stress-strain state in the vicinity of a concentrator such as dihedral angle. In: Voprosy svarochnogo proizvodstva (Questions of welding production), pp. 3–8. Chelyabinsk (1987)
88. Hasebe, N., Iida, J.: Intensity of corner and stress concentration factor. J. Eng. Mech. **109**(1), 346–356 (1983)
89. Hasebe, N., Kutanda, Y.: Calculation of stress intensity factors from stress concentration factor. Eng. Fract. Mech. **10**, 215–221 (1978)
90. Hasebe, N., Nakamura, T., Iida, J.: Notch mechanics for plane and thin plate bending problems. Eng. Fract. Mech. **37**(1), 87–99 (1990)
91. Hein, V., Erdogan, F.: Stress singularities in a two-material wedge. Int. J. Fract. Mech. **7**(3), 317–330 (1971)
92. Helsing, J., Jonsson, A.: On the computation of stress fields on polygonal domains with V-notches. Int. J. Numer. Methods Eng. **53**(2), 433–453 (2002)
93. Helsing, J., Ojala, R.: Corner singularities for elliptic problems: integral equations, graded meshes, quadrature, and compressed inverse preconditioning. J. Comput. Phys. **227**(20), 8820–8840 (2008)
94. Hills, D., Dini, D.: Characteristics of the process zone at sharp notch roots. Int. J. Solids Struct. **48**(14), 2177–2183 (2011)
95. Hufenbach, W., Kroll, L.: Stress analysis of notched anisotropic finite plates under mechanical and hygrothermal loads. Arch. Appl. Mech. **69**(3), 145–159 (1999)
96. Huth, J.H.: The complex-variable approach to stress singularities. J. Appl. Mech. **20**, 561–562 (1953)
97. Hwu, C., Kuo, T.L.: A unified definition for stress intensity factors of interface corners and cracks. Int. J. Solids Struct. **44**(18), 6340–6359 (2007)
98. Irwin, G.R.: Fracture. In: Flügge, S. (ed.) Encyclopedia of Physics. Elasticity and Plasticity, vol. 6, pp. 551–590. Springer, Berlin (1958)
99. Johnston, P.R., Elliott, D.: A sinh transformation for evaluating nearly singular boundary element integrals. Int. J. Numer. Methods Eng. **62**, 564–578 (2005)
100. Ju, S.: Finite element calculation of stress intensity factors for interface notches. Comput. Meth. Appl. Mech. Eng. **199**(33), 2273–2280 (2010)
101. Ju, S.H.: Calculation of notch H-integrals using image correlation experiments. Exp. Mech. **50**(4), 517–525 (2010)
102. Ju, S.H., Chung, H.Y., Jhao, B.J.: Experimental calculation of mixed-mode notch stress intensity factors for anisotropic materials. Eng. Fract. Mech. **76**(14), 2260–2271 (2009)
103. Ju, S.H., Chiu, C.Y., Jhao, B.J.: Determination of V-notch SIFs in multi-material anisotropic wedges by digital correlation experiments. Int. J. Solids Struct. **47**(7), 894–900 (2010)
104. Ju, S.H., Chung, H.Y., Liu, S.H.: Determining 2D notch SIFs by the image-correlation method. J. Chin. Inst. Eng. **34**(4), 503–514 (2011)
105. Kalandiya, A.I.: Remarks on the singularity of elastic solutions near corners. J. Appl. Math. Mech. **33**(1), 127–131 (1969)
106. Karp, S.N., Karal, F.C.J.: The elastic-field behaviour in the neighbourhood of a crack of arbitrary angle. Commun. Pure Appl. Math. **15**(4), 413–421 (1962)
107. Kazberuk, A.: Stress concentration around an oval hole. Acta Mech. Autom. **1**, 25–30 (2007)

108. Kazberuk, A.: Determining parameters of fracture toughness of quasibrittle materials using specimens with notches. Acta Mech. Autom. **3**(3), 28–31 (2009)
109. Kazberuk, A.: Stress intensity factors for cracks at the vertex of a rounded V-notch. Mater. Sci. **45**(5), 676–687 (2009)
110. Kazberuk, A.: Dwuwymiarowe zagadnienia mechaniki pękania ciał z karbami (Two-dimensional problems of fracture mechanics of bodies with notches). Bialystok University of Technology, Bialystok (2010)
111. Kazberuk, A., Niedźwiedź, M.: Stress distribution on the edge of a rounded v-shaped notch. In: Proceedings of the V International Symposium on Damage Mechanisms in Materials and Structures. Białystok, pp. 56–58 (2009)
112. Kazberuk, A., Niedźwiedź, M.: The influence of the shape of the notch on stress distribution on the boundary. Acta Mech. Autom. **3**(1), 38–41 (2009)
113. Kazberuk, A., Savruk, M.P.: Selected problems of fracture mechanics of bodies with V-notches. In: Fatigue and Fracture Mechanics: Proceedings of the XXIII Symposium University Technology and Life Sciences, Bydgoszcz, pp. 67–68 (2010)
114. Kazberuk, A., Savruk, M.P.: Stress concentration in vertexes of notches in complex stress states. In: Proceedings of the XIII Conference on Fracture Mechanics, Opole, pp. 104–106 (2011)
115. Kazberuk, A., Savruk, M.P., Tarasiuk, G.: Concentration of stresses in the rounded corners of the notches and holes under antiplane deformation. In: Fatigue and Fracture Mechanics: Proceedings of the XXIV Symposium on University of Technology and Life Sciences. Bydgoszcz, pp. 69–70 (2012)
116. Keer, L.M., Chantaramungkorn, K.: An elastic half plane weakened by a rectangular trench. J. Appl. Mech. **42**(3), 683–687 (1975)
117. Kim, J.K., Cho, S.B.: An analysis of eigenvalues and eigenvectors for V-notched cracks in pseudo-isotropic dissimilar materials. Int. J. Korean Soc. Precis. Eng. **3**(2), 33–44 (2002)
118. Klusák, J., Knésl, Z.: Determination of crack initiation direction from a bi-material notch based on the strain energy density concept. Comput. Mater. Sci. **39**(1), 214–218 (2007)
119. Klusák, J., Knésl, Z.: Reliability assessment of a bi-material notch: strain energy density factor approach. Theor. Appl. Fract. Mech. **53**(2), 89–93 (2010)
120. Klusák, J., Profant, T., Kotoul, M.: A comparison of two direct methods of generalized stress intensity factor calculations of bi-material notches. Key Engineering Materials, vol. 385, pp. 409–412. Trans Tech Publications (2008)
121. Knésl, Z., Klusák, J., Náhlık, L.: Crack initiation criteria for singular stress concentrations, part i: a universal assesment of singular stress concentrations. Eng. Mech. **14**(6), 399–408 (2007)
122. Knésl, Z., Klusák, J., Náhlık, L.: Crack initiation criteria for singular stress concentrations, part ii: stability of sharp and bimaterial notches. Eng. Mech. **14**(6), 409–422 (2007)
123. Koshelev, V., Ghassemi, A.: Wedge boundary elements for 2D problems with corner points. Eng. Anal. Bound. Elem. **32**(2), 168–175 (2008)
124. Kouzniak, N.V., Rossmanith, H.P., Savruk, M.P.: Plastic strain distribution near a tip of a sharp V-notch in a power hardening material. Mechanism and Mechanics of Damage and Failure, pp. 355–360. EMAS, London (1996)
125. Kouznyak, N.V., Rossmanith, H.P., Savruk, M.P.: Singular stresses at a tip of a sharp notch in power hardening materials under anti-symmetric load. Mater. Sci. **31**(6), 693–701 (1995)
126. Kuang, Z.B., Xu, X.P.: Singular behavior of a sharp V-notsh tip in power hardening material. In: Sih G.C., Nisitani H., Ishihara T. (eds.) Role of Fracture Mechanics in Modern Technology, pp. 477–484. Elsevier, Netherlands (1987)
127. Kuang, Z.B., Xu, X.P.: Stress and strain fields at the tip of a sharp V-notch in a power-hardening material. Int. J. Fract. **35**(1), 39–53 (1987)
128. Kullmer, G.: Elastic stress fields in the vicinity of a narrow notch with circular root. In: Proceedings of the European Conference on Reliability and Structural Integrity of Advanced Materials, ECF 9, Varna, Bulgary, vol. 2, pp. 905–910 (1992)

129. Kullmer, G., Richard, H.A.: Influence of the root radius of crack-like notches on the fracture load of brittle components. Arch. Appl. Mech. **76**, 711–723 (2006)
130. Labossiere, P.E.W., Dunn, M.L.: Calculation of stress intensities at sharp notches in anisotropic media. Eng. Fract. Mech. **61**(5–6), 635–654 (1998)
131. Labossiere, P.E.W., Dunn, M.L.: Stress intensities at interface corners in anisotropic bimaterials. Eng. Fract. Mech. **62**(6), 555–576 (1999)
132. Lazzarin, P., Filippi, S.: A generalized stress intensity factor to be applied to rounded V-shaped notches. Int. J. Solids Struct. **43**(9), 2461–2478 (2006)
133. Lazzarin, P., Tovo, R.: A unified approach to the evaluation of linear elastic stress fields in the neibourhood of cracs and notches. Int. J. Fract. **78**(1), 3–19 (1996)
134. Lazzarin, P., Zambardi, R.: The equivalent strain energy density approach re-formulated and applied to sharp V-shaped notches under localized and generalized plasticity. Fatigue Fract. Eng. Mater. Struct. **25**(10), 917–928 (2002)
135. Lazzarin, P., Tovo, R., Filippi, S.: Elastic stress distributions in finite size plates with edge notches. Int. J. Fract. **91**(3), 269–282 (1998)
136. Lazzarin, P., Zappalorto, M., Berto, F.: Generalised stress intensity factors for rounded notches in plates under in-plane shear loading. Int. J. Fract. **170**(2), 123–144 (2011)
137. Lebedev, D.F.: Brittle fracture of the composite elastic plane with a V-shaped notch. Proc. Natl. Acad. Sci. Armen. Mech. **43**(2), 12–22 (1990)
138. Li, J., Zhang, X.B., Recho, N.: Stress singularities near the tip of a two-dimensional notch formed from several elastic anisotropic materials. Int. J. Fract. **107**(4), 379–395 (2001)
139. Li, Y., Song, M.: Method to calculate stress intensity factor of V-notch in bi-materials. Acta Mech. Solida Sinica **21**(4), 337–346 (2008)
140. Lin, K.Y., Tong, P.: Singular finite elements for the fracture analysis of V-notched plate. Int. J. Numer. Methods Eng. **15**(9), 1343–1354 (1980)
141. Lin, S., Hills, D.A.: Stress intensity factors for cracks emanating from a semicircular notch in a half-plate. J. Strain Anal. **31**(6), 433–439 (1996)
142. Livieri, P.: A new path independent integral applied to notched components under mode I loading. Int. J. Fract. **123**(3–4), 107–125 (2003)
143. Livieri, P., Segala, F.: Analytical evaluation of J-integral for elliptical and parabolic notches under mode I and mode II loading. Int. J. Fract. **148**(1), 57–71 (2007)
144. Livieri, P., Segala, F.: Evaluation of stress intensity factors from elliptical notches under mixed mode loadings. Eng. Fract. Mech. **81**, 110–119 (2012)
145. Loghin, A., Joseph, P.F.: Asymptotic solutions for mixed mode loading of cracks and wedges in power law hardening materials. Eng. Fract. Mech. **68**(14), 1511–1534 (2001)
146. Lum, C., Foschi, R.O.: Arbitrary V-notches in orthotropic plates. J. Eng. Mech. **114**(4), 638–655 (1988)
147. Maz'ya, V.G., Soloviev, A.A.: Boundary integral equations on contours with peaks. Birkhäuser, Boston (2010)
148. Mikhailov, S.E.: On a plane problem for the two connected anisotropic wedges. Mech. Solids **13**(4), 155–160 (1978)
149. Mikhailov, S.E.: The asymptotic behavior of solutions of some integral equations and plane elasticity problems near the corners under given stresses on the boundary. Mech. Solids **24**(3), 33–43 (1989)
150. Mitra, A.K., Ingber, M.S.: A multiple-node method to resolve the difficulties in the boundary integral equation method caused by corners and discontinuous boundary conditions. Int. J. Numer. Methods Eng. **36**(10), 1735–1746 (1993)
151. Mohammed, I., Liechti, K.M.: The effect of corner angles in bimaterial structures. Int. J. Solids Struct. **38**(24), 4375–4394 (2001)
152. Munz, D., Yang, Y.Y.: Stresses near the edge of bonded dissimilar materials described by two stress intensity factors. Int. J. Fract. **60**(2), 169–177 (1993)
153. Muskhelishvili, N.I.: Some Basic Problems of the Mathematical Theory of Elasticity, 2nd edn. Noordhoff International Publishing, Leyden (1977)

154. Nachname, M., Hohe, J., Becker, W., et al.: A closed-form analysis of material and geometry effects on stress singularities at unsymmetric bimaterial notches. Proc. Appl. Math. Mech. **2**(1), 210–211 (2003)
155. Neskorodev, N.M., Neskorodev, R.N.: Stress singularities in the neighborhood of corners of orthotropic plates. J. Math. Sci. **101**(1), 2785–2788 (2000)
156. Neuber, H.: Die halbeelliptische Kerbe mit Riß als Beispiel zur Korrelation von Mikro- und Makrospannungskonzentrationen. Ing.-Arch. **46**, 389–399 (1977)
157. Nisitani, H.: The two-dimensional stress problem solved using an electric digital computer. Bull. JSME **11**(43), 14–23 (1968)
158. Nisitani, H.: Solutions of notch problems by body force method. In: Sih, G.C. (ed.) Stress Analysis of Notch Problems. Mechanics of Fracture, vol. 5, pp. 1–68. Noordhoff International Publishing, Alphen aan den Rijn (1978)
159. Niu, Z., Ge, D., Cheng, C., Ye, J., Recho, N.: Evaluation of the stress singularities of plane V-notches in bonded dissimilar materials. Appl. Math. Model. **33**, 1776–1792 (2009)
160. Niu, Z.R., Recho, N., Yang, Z.Y., Cheng, C.Z.: Elastic-plastic stress singularities of plane V-notches in power-hardening materials. Key Eng. Mater. **465**, 105–110 (2011)
161. Noda, N.A., Oda, K., Inoue, T.: Analysis of newly-defined stress intensity factors for angular corners using singular integral equations of the body force method. Int. J. Fract. **76**(3), 243–261 (1996)
162. Nui, L.S., Chehimi, C., Pluvinage, G.: Stress field near a large blunted tip V-notch and application of the concept of the critical notch stress intensity factor (NSIF) to the fracture toughness of very brittle materials. Eng. Fract. Mech. **49**(3), 325–335 (1994)
163. Ovcharenko, Y.N.: Teoriya i praktika V-obraznykh vyrezov v mekhanike razrusheniya (Theory and practice of V-shaped notches in fracture mechanics). TSU, Tula (2003)
164. Ovcharenko, Y.N.: The elastic stress-strain state and strain energy density at the vertex of extremely narrow U-notches. Proc. Tula State Univ. Nat. Sci. **2**, 97–108 (2010)
165. Panasyuk, V.V., Savruk, M.P., Datsyshin, A.P.: Raspredeleniye napryazhenii okolo treshchin v plastinakh i obolochkakh (Stress distribution around cracks in plates and shells). Naukova dumka, Kyiv (1976)
166. Panasyuk, V.V., Savruk, M.P., Kazberuk, A.: Stress concentration near sharp and rounded V-notches. Mater. Sci. **49**(6), 711–722 (2014)
167. Parton, V.Z., Morozov, E.M.: Elastic-Plastic Fracture Mechanics. Mir, Moscow (1978)
168. Petkov, Z.B., Gospodinov, G.K.: Evaluation of fracture mechanics parameters for a general corner using a weight function method. Acta Mech. **93**, 145–155 (1992)
169. Ping, X.C., Chen, M.C., Xie, J.L.: Singular stress analyses of V-notched anisotropic plates based on a novel finite element method. Eng. Fract. Mech. **75**, 3819–3838 (2008)
170. Pluvinage, G.: Mekhanika uprugoplasticheskogo razrysheniya (Mechanics of elastic-plastic fracture). Mir, Moscow (1993)
171. Portela, A., Aliabadi, M.H., Rooke, D.P.: Efficient boundary element analysis of sharp notched plates. Int. J. Numer. Methods Eng. **32**, 445–470 (1991)
172. Prößdorf, S., Rathsfeld, A.: Quadrature and collocation methods for singular integral equations on curves with corners. Z. Anal. Anwendungen **8**(3), 197–220 (1989)
173. Providakis, C.P.: Boundary element analysis of creeping V-notched metallic plates in bending. Eng. Fract. Mech. **64**(2), 129–140 (1999)
174. Providakis, C.P.: Creep analysis of V-notched metallic plates: boundary element method. Theor. Appl. Fract. Mech. **32**(1), 1–7 (1999)
175. Qian, Z.Q.: On the evaluation of the free-edge stress intensity factors for a joint subjected to a uniform change in temperature. J. Therm. Stress. **23**(5), 463–481 (2000)
176. Qian, Z.Q.: On the evaluation of wedge corner stress intensity factors of bi-material joints with surface tractions. Comput. Struct. **79**(1), 53–64 (2001)
177. Qian, Z.Q., Akisanya, A.R.: Wedge corner stress behaviour of bonded dissimilar materials. Theor. Appl. Fract. Mech. **32**(3), 209–222 (1999)
178. Radaj, D., Zhang, S.: On the relations between notch stress and crack stress intensity in plane shear and mixed mode loading. Eng. Fract. Mech. **44**(5), 691–704 (1993)

179. Rao, A.K.: Stress concentrations and singularities at interface corners. ZAMM J. Appl. Math. Mech. **51**(5), 395–406 (1971)
180. Rice, J.R.: A path independent integral and the approximate analysis of strain concentrations by notches and cracks. J. Appl. Mech. **35**(2), 379–386 (1968)
181. Rooke, D.P., Baratta, F.I., Cartwright, D.J.: Simple methods of determining stress intensity factors. Eng. Fract. Mech. **14**(2), 397–426 (1981)
182. Rösel, R.: On the wedge/notch eigenvalue. Int. J. Fract. **33**(1), 61–71 (1987)
183. Rudge, M.R.H.: Interfacial stress singularities in a bimaterial wedge. Int. J. Fract. **63**(1), 21–26 (1993)
184. Rudge, M.R.H., Tiernan, D.M.: Interfacial stress singularities in a bimaterial wedge. Int. J. Fract. **74**(1), 63–75 (1995)
185. Rudge, M.R.H., Tiernan, D.M.: Stress singularities in composite wedge-shaped materials. Fatigue Fract. Eng. Mater. Struct. **22**(1), 11–15 (1999)
186. Rzasnicki, W., Mendelson, A.: Application of boundary integral method to elastoplastic analysis of V-notched beams. Int. J. Fract. **11**(2), 329–342 (1975)
187. Sargsyan, A.M.: On stress singularity in one problem of elasticity theory for the wedge. Proc. Natl. Acad. Sci. Armen. Mech. **61**(1), 48–53 (2008)
188. Savruk, M.P.: Dvumernyye zadachi uprugosti dla tel s treshchinami (Two-dimensional problems of elasticity for bodies with cracks). Naukova dumka, Kyiv (1981)
189. Savruk, M.P.: Koeficienty intensivnosti napryazhenii v telakh s treshchinami (Stress intensity factors in bodies with cracks). Naukova dumka, Kyiv (1988)
190. Savruk, M.P.: Solving planer problems of crack theory for regions with angular points. Mater. Sci. **24**(1), 39–49 (1988)
191. Savruk, M.P., Datsyshin, A.P.: Interaction between a system of cracks and the boundaries of an elastic body. Int. Appl. Mech. **10**(7), 755–761 (1974)
192. Savruk, M.P., Kazberuk, A.: Relationship between the stress intensity and stress concentration factors for sharp and rounded notches. Mater. Sci. **42**(6), 725–738 (2006)
193. Savruk, M.P., Kazberuk, A.: Stress concentration around a rounded notch for arbitrary vertex curvature. Acta Mech. Autom. **1**(1), 90–102 (2007)
194. Savruk, M.P., Kazberuk, A.: Stress intensity factors at the apex of the diamond hole in the stretched plane. In: Proceedings of the IV International Symposium on Damage Mechanisms in Materials and Structures, pp. 233–236. Bialystok (2007)
195. Savruk, M.P., Kazberuk, A.: Stress intensity factors at the apex of the diamond hole in the stretched plane. Acta Mech. Autom. **1**(2), 37–40 (2007)
196. Savruk, M.P., Kazberuk, A.: A unified approach to problems of stress concentration near V-shaped notches with sharp and rounded tip. Int. Appl. Mech. **43**(2), 182–197 (2007)
197. Savruk, M.P., Kazberuk, A.: A unified approach to the problem of the distribution of stresses near sharp and rounded V-shaped notches. In: Mhitarian, S.M. (ed.) Aktual'nye problemy mekhaniki sploshnoy sredy, pp. 359–363. Erevanskiy gos. un-t arhitektury i stroitel'stva, Erevan (2007)
198. Savruk, M.P., Kazberuk, A.: Plane periodic boundary-value problem of elasticity theory for a half-plane with curvilinear edge. Mater. Sci. **44**(4), 461–470 (2008)
199. Savruk, M.P., Kazberuk, A.: Problems of fracture mechanics of solid bodies with V-shaped notches. Mater. Sci. **45**(2), 162–180 (2009)
200. Savruk, M.P., Kazberuk, A.: Stress concentration problems for elastic domains with V-shaped notches. In: Panasyuk, V.V. (ed.) Mekhanika ruinuvannya materialiv i mitsnist' konstruktsii (Fracture mechanics of materials and strength of structures), pp. 75–86. Lviv (2009)
201. Savruk, M.P., Kazberuk, A.: Stresses in an elastic plane with a periodic system of closely located holes. Mater. Sci. **45**(6), 831–844 (2009)
202. Savruk, M.P., Kazberuk, A.: On some problems of fracture mechanics in bodies with sharp and rounded V-notches. Acta Mech. Autom. **4**(2), 113–123 (2010)
203. Savruk, M.P., Kazberuk, A.: Two-dimensional fracture mechanics problems for solids with sharp and rounded V-notches. Int. J. Fract. **161**, 79–95 (2010)

204. Savruk, M.P., Kazberuk, A.: Antisymmetric stress distribution in an elastic body with a sharp or a rounded V-shaped notch. Mater. Sci. **46**(6), 711–722 (2011)
205. Savruk, M.P., Kazberuk, A.: Distribution of stresses near V-shaped notches in the complex stressed state. Mater. Sci. **47**(4), 476–487 (2012)
206. Savruk, M.P., Osiv, P.M.: Numerical solution of the singular integral equations for plain problems of the theory of cracks with angular points on the boundary contours. Mater. Sci. **25**(3), 294–301 (1989)
207. Savruk, M.P., Zelenyak, V.M.: Dvovymirni zadachi termopruzhnosti dla kuskovo-odnoridnykh til z trishchynamy (Two-dimensional problem of thermoelasticity for piecewise homogeneous bodies with cracks). Rastr-7, Lviv (2009)
208. Savruk, M.P., Osiv, P.M., Prokopchuk, I.V.: Chislennyy analiz v ploskikh zadachakh teorii treshchin (Numerical analysis in plane problems of theory of cracks). Naukova dumka, Kyiv (1989)
209. Savruk, M.P., Shkarayev, S.V., Madenci, E.: Stress near apex of dissimilar material with bilinear behavior. Theor. Appl. Fract. Mech. **31**(3), 203–212 (1999)
210. Savruk, M.P., Kazberuk, A., Niedźwiedź, M.: Stress distribution around sharp and rounded corners notches for complex stress state. Matematychni problemy mekhaniky neodnoridnykh struktur (Mathematical problems of mechanics of nonhomogeneous structures), pp. 81–83. Lviv (2010)
211. Savruk, M.P., Kazberuk, A., Tarasiuk, G.: Distribution of stresses over the contour of rounded V-shaped notch under antiplane deformation. Mater. Sci. **47**(6), 717–725 (2012)
212. Savruk, M.P., Kazberuk, A., Tarasiuk, G.: Stress concentration near holes in the elastic plane subjected to antiplane deformation. Mater. Sci. **48**(4), 415–426 (2013)
213. Seweryn, A.: Asymptotic methods of determining stress intensity factors for V-notches in plane problems in the theory of elasticity. Rozprawy Inżynierskie (Eng. Trans.) **38**, 467–486 (1990)
214. Seweryn, A.: Modeling distributions of stresses and displacements in the vicinity of the V-notch apex in plane problems in the theory of elasticity - I. Rozprawy Inżynierskie (Eng. Trans.) **38**, 351–376 (1990)
215. Seweryn, A.: Modeling distributions of stresses and displacements in the vicinity of the V-notch apex in plane problems in the theory of elasticity - II. Rozprawy Inżynierskie (Eng. Trans.) **38**, 377–396 (1990)
216. Seweryn, A.: Kumulacja uszkodzeń i pękanie elementów konstrukcyjnych w złożonych stanach obciążeń (Accumulation of damage and fracture of structural elements in complex states of loading). Bialystok University of Technology, Bialystok (1997)
217. Seweryn, A.: Modeling of singular stress fields using finite element method. Int. J. Solids Struct. **39**(18), 4787–4804 (2002)
218. Seweryn, A.: Metody numeryczne w mechanice pekania (Numerical methods in fracture mechanics). Institute of Fundamental Technological Research. Polish Academy of Sciences, Warsaw (2003)
219. Seweryn, A., Adamowicz, A.: Modelling of stress fields in the elements with cracks and sharp notches. Przeglad Mechaniczny (Mech. Rev.) **1**, 36–41 (2002)
220. Seweryn, A., Adamowicz, A.: On analytic constraints and elements methods in modeling stresses near the tips of cracks and V-notches. Mater. Sci. **41**(4), 462–478 (2005)
221. Seweryn, A., Łukaszewicz, A.: Numerical modeling methods of problems of linear fracture mechanics. Przeglad Mechaniczny (Mech. Rev.) **5–6**, 36–42 (2000)
222. Seweryn, A., Molski, K.: Elastic stress singularities and corresponding generalized stress intensity factors for angular corners under various boundary conditions. Eng. Fract. Mech. **55**(4), 529–556 (1996)
223. Shin, K.C., Kim, W.S., Lee, J.J.: Application of stress intensity to design of anisotropic/isotropic bi-materials with a wedge. Int. J. Solids Struct. **44**(24), 7748–7766 (2007)
224. Sih, G.C.: Strain-energy-density factor applied to mixed mode crack problems. Int. J. Fract. **10**(3), 305–321 (1974)

225. Sih, G.C., Liebowitz, H.: Mathematical theories of brittle fracture. In: Liebowitz, H. (ed.) Fracture, vol. 2, pp. 67–190. Academic Press, New York (1968)
226. Sinclair, G.B.: A remark on the determtnation of mode I and mode II stress intensity factors for sharp re-entrant corners. Int. J. Fract. **27**(3), 81–85 (1985)
227. Sinclair, G.B., Okajima, M., Griffin, J.M.: Path independent integrals for computing stress intensity factors at sharp notches in elastic plates. Int. J. Numer. Methods Eng. **20**, 999–1008 (1984)
228. Song, C., Tin-Loi, F., Gao, W.: A definition and evaluation procedure of generalized stress intensity factors at cracks and multi-material wedges. Eng. Fract. Mech. **77**(12), 2316–2336 (2010)
229. Strandberg, M.: A numerical study of the elastic stress field arising from sharp and blunt V-notches in SENT-specimen. Int. J. Fract. **100**(4), 329–342 (1999)
230. Szabó, B.A., Yosibash, Z.: Numerical analysis of singularities in two dimensions. Part 2: computation of generalized flux/stress intensity factors. Int. J. Numer. Methods Eng. **39**(3), 409–434 (1996)
231. Teh, L.S., Brennan, F.P.: Evaluation of mode I stress intensity factors for edge cracks from 2-D V-notches using composition of constituent SIF weight functions. Int. J. Fatigue **29**(7), 1253–1268 (2007)
232. Teh, L.S., Love, A.J., Brennan, F.P.: Mode I stress intensity factors for edge cracks emanating from 2-D U-notches using composition of SIF weight functions. Int. J. Fatigue **28**(4), 355–365 (2006)
233. Theocaris, P.S.: The order of singularity at a multi-wedge corner of a composite plate. Int. J. Eng. Sci. **12**(2), 107–120 (1974)
234. Theocaris, P.S., Ioakimidis, N.I.: The V-notched elastic half-plane problem. Acta Mech. **32**(1–3), 125–140 (1979)
235. Tur, M., Fuenmayor, J., Mugadu, A., Hills, D.A.: On the analysis of singular stress fields. Part 1: finite element formulation and application to notches. J. Strain Anal. **37**(5), 437–444 (2002)
236. Ufland, Y.S.: Integral'nye preobrazovaniya v zadachakh teorii uprogosti (Integral transforms in problems of the theory of elasticity). Nauka, Moscow (1967)
237. Ushijima, K., Chen, D.H., Kitte, N.: Intensity of a plastic singular stress field at the notch tip. JSME Int. J. A Solid Mech. Mater. Eng. **45**(2), 170–176 (2002)
238. Vable, M., Maddi, J.R.: Boundary element analysis of inclusions with corners. Eng. Anal. Bound. Elem. **31**(9), 762–770 (2007)
239. Vorovich, I.I.: On some problems of stress concentration. Kontsentratsiya napryazheniy (Stress concentration), vol. 2, pp. 45–53. Naukova dumka, Kyiv (1968)
240. Vorovich, I.I.: Formulation of boundary-value problems in the theory of elasticity for an infinite energy integral and basic properties of homogeneous solutions. Mekhanika deformiruyemykh tel i konstruktsii (Mechanics of solids and structures), pp. 112–128. Mashinostroyeniye, Moskow (1975)
241. Wang, W., Kuang, Z.: Higher order asymptotic fields at the tip of a sharp V-notch in a power-hardening material. Acta. Mech. Solida Sinica **15**(2), 102–110 (2002)
242. Wieghardt, K.: über das spalten und zerreißen elastischer körper. Z. Math. Phys. **55**(2), 60–103 (1907)
243. Williams, M.L.: Stress singularities resulting from various boundary conditions in angular corners of plates in extension. J. Appl. Mech. **19**(4), 526–530 (1952)
244. Williams, M.L.: The complex variable approach to stress singularities. J. Appl. Mech. **23**, 477–478 (1956)
245. Wu, K.C., Chang, F.T.: Near-tip fields in a notched body with dislocations and body forces. J. Appl. Mech. **60**(4), 936–941 (1993)
246. Wu, K.C., Chen, C.T.: Stress analysis of anisotropic elastic V-notched bodies. Int. J. Solids Struct. **33**(17), 2403–2416 (1996)
247. Wu, Z., Liu, Y.: Analytical solution for the singular stress distribution due to V-notch in an orthotropic plate material. Eng. Fract. Mech. **75**(8), 2367–2384 (2008)

248. Wu, Z., Liu, Y.: Asymptotic fields near an interface corner in orthotropic bi-materials. Int. J. Fract. **156**(1), 37–51 (2009)
249. Wu, Z., Liu, Y.: Singular stress field near interface edge in orthotropic/isotropic bi-materials. Int. J. Solids Struct. **47**(17), 2328–2335 (2010)
250. Xia, L., Wang, T.C.: Singular behaviour near the tip of a sharp V-notch in a power law hardening material. Int. J. Fract. **59**(1), 83–93 (1993)
251. Xu, J.Q., Liu, Y.H., Wang, X.G.: Numerical methods for the determination of multiple stress singularities and related stress intensity coefficients. Eng. Fract. Mech. **63**(6), 775–790 (1999)
252. Xu, X.X., Cai, Q.G., Su, Y., Ma, W.D.: Notch root strain and stress distributions in power hardening materials. Int. J. Fract. **41**(4), 275–282 (1989)
253. Yang, S., Chao, Y.J.: Asymptotic deformation and stress fields at the tip of a sharp notch in an elastic-plastic material. Int. J. Fract. **54**(3), 211–224 (1992)
254. Yosibash, Z., Schiff, B.: A superelement for two-dimensional singular boundary value problems in linear elasticity. Int. J. Fract. **62**(4), 325–340 (1993)
255. Yosibash, Z., Schiff, B.: Superelements for the finite element solution of two-dimensional elliptic problems with boundary singularities. Finite Elem. Anal. Des. **26**(4), 315–335 (1997)
256. Yosibash, Z., Szabó, B.: Numerical analysis of singularities in two-dimensions part 1: computation of eigenpairs. Int. J. Numer. Methods Eng. **38**(12), 2055–2082 (1995)
257. Yosibash, Z., Szabó, B.A.: Generalized stress intensity factors in linear elastostatics. Int. J. Fract. **72**(3), 223–240 (1995)
258. Yosibash, Z., Szabó, B.A.: A note on numerically computed eigenfunctions and generalized stress intensity factors associated with singular points. Eng. Fract. Mech. **54**(4), 593–595 (1996)
259. Yu, T., Shi, L.: Determination of sharp V-notch stress intensity factors using the extended finite element method. J. Strain Anal. **47**(2), 95–103 (2012)
260. Yuan, H.: Singular stress fields at V-notch tips in elastoplastic pressure-sensitive materials. Acta Mech. **118**(1–4), 151–170 (1996)
261. Yuan, H., Lin, G.: Analysis of elastoplastic sharp notches. Int. J. Fract. **67**(3), 187–216 (1994)
262. Zargaryan, S.S.: Plane elasticity problem for simply connected domains with corners for given external forces on the boundary. Rep. Acad. Sci. Armen. SSR **60**(1), 43–50 (1975)
263. Zargaryan, S.S.: Singularities of solutions of a system of singular integral equations in plane elasticity theory for given stresses on the boundary. Rep. Acad. Sci. Armen. SSR **77**(4), 167–172 (1983)
264. Zargaryan, S.S., Maz'ya, V.G.: The asymptotic form of the solutions of the integral equations of potential theory in the neighbourhood of the corner points of a contour. J. Appl. Math. Mech. **48**(1), 120–124 (1984)
265. Zhang, N., Joseph, P.F.: A nonlinear finite element eigenanalysis of singular plane stress fields in bimaterial wedges including complex eigenvalues. Int. J. Fract. **90**(3), 175–207 (1998)
266. Zhang, S.W., Chen, Y.Z., Lin, W.Z.: Investigation of shear stress distribution in notch problem under sliding mode case. Int. J. Fract. **56**(1), 85–92 (1992)
267. Zhu, H., Xu, J., Feng, M.: Singular fields near a sharp V-notch for power law creep material. Int. J. Fract. **168**(2), 159–166 (2011)

http://www.springer.com/978-3-319-44554-0

Stress Concentration at Notches
Savruk, M.P.; Kazberuk, A.
2017, XVIII, 498 p. 207 illus., Hardcover
ISBN: 978-3-319-44554-0